

1 **Response to Reviewer 1’s comments**

2  
3 We thank Reviewer 1 for the time to go through our manuscript in details. This manuscript  
4 describes a new and efficient method to produce a physical TC event set in the western North  
5 Pacific basin. In general, reviewers think after careful revision, the results of this study is of  
6 great interest and relevance, and it will be a useful contribution to the field of TC occurrence  
7 risk assessment. Here is our point-to-point response to Reviewer 1’s comments. Reviewer 1’s  
8 comments are in red.

9  
10 **Response to Major Issues**

11  
12 *You have explained that you only used 6-hourly surface wind speed (i.e., lines 67-69 and*  
13 *discussed in Section 4.2 as well), is your risk assessment model able to comprehend a full TC*  
14 *risk? What about TC-rainfall (you only mentioned about it in the last 2-3 sentences in*  
15 *Conclusions) and TC-induced storm surge, which are more significant than winds in many*  
16 *regions of the world. For example, the recent Hurricane Florence in USA and Mangkut in*  
17 *South China caused significant damaged due to surge and rainfall, respectively. Therefore,*  
18 *under such circumstances, what is the applicability of your proposed approach? You need to*  
19 *think about the generalization, replicability, and adoptability of your approach from a wider*  
20 *perspective and not only from the study area.*

21  
22 We are thankful for the reviewer’s comment to the overall impact of Typhoons and their  
23 differentiated reasoning in form of the different meteorological variables concerned. In this  
24 study, we present a method, which addresses the basic, critical issue in typhoon risk  
25 assessments – a robust methodology to determine the real frequency of a tropical cyclone (TC)  
26 occurrence with high socioeconomic impact *potential*. We are doing so by automatically  
27 identify and tracking severe, damage relevant tropical cyclones in a data set being  
28 representative of several thousand years of “observations”, the TIGGE archive. Based on the  
29 large amount of data from the different multi-model multi-member ensembles to be analysed,  
30 in this study, we use thus a computationally inexpensive approach: by applying an impact-  
31 oriented tracking algorithm WiTRACK (Leckebusch et al., 2008; Kruschke, 2015; Befort et al.,  
32 2020) on multi-model ensemble forecasts to generate a large, physical consistent TC event set.  
33 This *identification* of major events is thus based on one meteorological variable only (wind  
34 speed), but is capable of identifying events of *general* loss relevance. We recently demonstrated  
35 in Befort et al. (2020) that the tracking algorithm used in this study (WiTRACK), can  
36 automatically identify the relevant (over 90%) of TCs with high overall socioeconomic impact  
37 (e.g., above 3,000 million RMB or 440 million US\$ to mainland China). This implies the event  
38 set generated by our approach is in principle suitable for general TC risk assessments, as well  
39 as for an assessment of the hazards frequency-intensity distribution specifically. As we fully  
40 agree with Reviewer 1 that TC-rainfall and TC-induced storm surge are also important factors  
41 in assessing the full impact (risk) of TC to society, we would like to point out that the events  
42 identified and used in this study are including those where potential loss is caused not only by

43 the direct wind force but also by secondary natural hazards, e.g. flooding by precipitation, or  
44 potential storm surge by the combined wind and pressure impact.

45 Therefore, the applicability of our proposed approach is directly visible and fundamental.  
46 While studies like e.g. Sajjad and Chan (2019) are focussing on an overall assessment of  
47 integrated risks (hazard x vulnerability/resilience; further comments to this topic, please find  
48 below) based on observed tracks from only some 60-70 years (of inhomogeneous data of  
49 different quality), our approach utilizes data (in this case multi-model synoptic forecasts)  
50 representative of ~10k years. To quantify robustly the probability of occurrence of e.g., a 100-  
51 year event from 60-70 years of observations is widely impossible (because it may potentially  
52 not have realised during this short observational period). Consequently, such an approach is  
53 not used e.g., in industry applications and is only of limited use for risk assessments as the  
54 **underlying** hazard component probability distribution is not sufficiently known.

55 The reviewer mentioned the topic of “*generalization, replicability, and adoptability*”. We fully  
56 agree and this is exactly the reason why we developed this approach.

- 57 • By using an impact-based identification of the natural hazard relative to the datasets  
58 typical characteristics (i.e., the 98<sup>th</sup> percentile of surface-near wind speeds), the  
59 assessment of the hazard is accounting of potential biases in the data set under  
60 investigation (e.g., AOGCM, NWP, or RCM simulations) and is linked to overall losses  
61 out of those events relative to the climatological distribution of these data sets.
- 62 • By utilizing ensemble forecasts (i.e., TIGGE’s unrealised TC events), we secure the  
63 statistical robustness of our intensity-frequency distribution assessment to create an  
64 event-set being representative of the risk of occurrence of events of potentially  
65 damaging characteristic (so called tail events).

66 We have demonstrated the applicability and transferability of this approach in several studies  
67 for different hazards and different regions (e.g. Leckebusch et al., 2008; Nissen et al.,  
68 2014; Osinski et al., 2016; Befort et al., 2015; Befort et al., 2016; Befort et al., 2019; Walz and  
69 Leckebusch, 2019)

70 A more in-depth investigation of the contribution of different drivers (e.g., extreme  
71 precipitation and storm surges) of loss and damage during a (non-realised) severe TC event  
72 would be beyond the scope of this study. Nevertheless, once a representative TC event set is  
73 derived, which provides robust information of the frequency of high impact TCs, the impact of  
74 extreme precipitation and storm surges could be integrated e.g., following the approach  
75 developed and published by us in Befort et al. (2015). **We have included the above**  
76 **information in Sect. 5 summary for clarity.**

77

78 *Recently, Sajjad and Chan 2019 and Sajjad et al. 2020 proposed typhoon risk frameworks*  
79 *based on TC hazard (wind-based similar to yours), vulnerability, and disaster resilience, which*  
80 *provides a comprehensive information on TC risk. They found that the Pearl River delta region*  
81 *in Guangdong (area primarily mentioned in your case, Line) is a statistically significant*  
82 *hotspot of TC risk. How do you see the usefulness of your method for such frameworks? A*  
83 *thorough discussion regarding this is necessary*

84 *Similarly, most of the discussion in the manuscript revolves around TC-hazard and neglects*  
85 *the vulnerability and resilience within the regions where TCs are making landfalls. For*  
86 *instance, you say on Lines 236-238 that overall impacts of a storm is related to many factors*  
87 *such as size, duration, and intensity. However, the impacts are not only related to TC-*  
88 *associated factors but vulnerability and resilience are also integral parts of overall impacts*  
89 *and risks associated with TCs, as discussed in Sajjad and Chan 2019 and Sajjad et al. 2020.*  
90 *How do you incorporate these characteristics within the TC risk discussion of yours?*

91

92 We think Reviewer 1 may have misread the purpose of our study because we do not share the  
93 same definition of the term “risk”. The term “risk” in this study refers to the possibility of  
94 occurrence of an event (e.g. Vickery et al., 2000; Emanuel et al., 2006), as outlined in the title.  
95 In the context of the papers cited by Reviewer 1, this manuscript focuses on the hazard  
96 component in the framework of a classical impact modelling and assessment approach. Please  
97 note that in terms of an impact modelling approach, the components would be the hazard (and  
98 its risk of occurrence), the vulnerability (which would include measures of resilience), and the  
99 exposure of values at risk. **We have replaced the term “risk” by “hazard” in relevant**  
100 **places in the manuscript to make this point clearer.** To avoid confusion, hereinafter, we  
101 use the term “hazard” to represent the possibility of occurrence of a natural event; and the term  
102 “risk” to reflect a systemic integrated perspective of resultant impacts by the combination of  
103 information about the hazard, the vulnerability, and the exposure. This terminology would be  
104 more similar to the approach used in Sajjad and Chan (2019) and Sajjad et al. (2020), and will  
105 also account for the common practice in industry applications (e.g., CAT models).

106

107

108 *Additionally, you need to detail the current limitations of your method. For example, how well*  
109 *this method could perform at higher resolution assessments, which are more important for*  
110 *policy and decision-making in the context of DRR efforts? What are the future prospects of*  
111 *your study?*

112

113 Many thanks for this comment. In comparison to other methods to generate large TC event sets,  
114 our specific approach is **limited** mainly by the source of data used. The current TC event set  
115 constructed on synoptic scale forecasts archived in TIGGE, is strictly spoken representative  
116 only for the current climate state. Any longer-term climate variability (e.g. multi-decadal  
117 fluctuations like the PDO) and their impacts on any TC frequency-intensity distribution are not  
118 accounted for in this setting. Nevertheless, the presented approach would be equally applicable  
119 to data sets representing that kind of variability on longer time scales (e.g. decadal predictions  
120 or transient climate model simulations). Another limitation is obviously that we do not account  
121 for a direct assessment of the damage (loss) contribution of individual meteorological variables  
122 (e.g., precipitation leading to flooding, as mentioned above). **We added a specific section on**  
123 **limitations in Sect. 5 [Lines 441-447].**

124 It is not fully clear what Reviewer 1 refers to as “**higher resolution assessments**”. The TIGGE  
125 archive provides forecast data on a spatial scale ( $\sim 0.56^\circ - 1.25^\circ$ ), which is not matched by any  
126 other data source of comparable length (equivalent to 10k years of observations of TCs).

127 Further, we intentionally linked our (forecast) model based assessment to in-situ point  
128 observations from stations: the ultimate downscaling test. As we have demonstrated in section  
129 4.3, one of the potential applications of our event set is to improve the return-period/return  
130 level calculation of the wind hazard at the local scale. Wind speed values are used in practice  
131 to decide on payments out of e.g. parametric insurance products (Swiss Re, 2016).  
132 Consequently, reliable wind-based trigger points of typhoon parametric insurance can be  
133 determined. This will further improve the suitability and flexibility of parametric insurance for  
134 DRR applications. Ultimately, this will improve the speed of post-disaster recovery. **We**  
135 **added a respective paragraph to the discussion [Lines 360-364, Lines 469-477].**

136 With regard to **future prospects** of this study, we discuss this in Section 5. In particular, unlike  
137 event sets generated from a stochastic approach, the TC-associated precipitation field is  
138 simulated directly by the model. This means a more complex compound TC hazard assessment,  
139 as mentioned above (limitations), can be done as well in principle. The event set that we have  
140 constructed contains all necessary information for applications in the DRR context. Once  
141 robust trigger points for the local hazard are available (including their uncertainty), the targeted  
142 application of parametric products in disaster relief application is possible. Especially, when it  
143 comes to the evaluation of the basis risk (the risk not covered by payments out of a parametric  
144 product). This study is merely the first step toward a statistically robust, full physical model  
145 based TC hazard assessment. **We added a respective paragraph to Sect. 5 [Lines 469-477].**

146

#### 147 *Specific Comments*

148 *Lines 10-13: The sentence is long and it is difficult to follow. Would be better to break it into*  
149 *two sentences, if possible.*

150

151

152 We thank Reviewer 1 for pointing this out, **we have modified this sentence accordingly.**

153

154

155 *Line 22: There is no such thing as “natural disaster” but only natural hazards. Disasters*  
156 *always involve human agency. Therefore, please avoid using this term and check the*  
157 *manuscript thoroughly for this issue. For further details, you are encouraged to see*  
158 *[https://www.undp.org/content/undp/en/home/blog/2017/5/18/Natural-disasters-don-t-exist-](https://www.undp.org/content/undp/en/home/blog/2017/5/18/Natural-disasters-don-t-exist-but-natural-hazards-do.html)*  
159 *[but-natural-hazards-do.html](https://www.undp.org/content/undp/en/home/blog/2017/5/18/Natural-disasters-don-t-exist-but-natural-hazards-do.html)*

160

161

162 Many thanks for pointing this out. Although we agree in principle that the disaster aspect  
163 includes a men-made perspective in its impact on human influenced structures the personal  
164 position expressed in this blog is document of a narrow understanding and perspective of nature.  
165 A natural hazard can be a disaster for the environment, even without human influences.  
166 Following good scientific practice, we prefer to use peer-reviewed literature for scientific  
167 studies and not personal comments. We used the phrase “natural disaster” as a generic term to  
168 indicate a natural event with sudden, large negative economic or environmental losses. The  
169 definition of “disaster” that we used here is similar to the definition stated in the IFRC webpage  
170 (see [https://www.ifrc.org/en/what-we-do/disaster-management/about-disasters/what-is-a-](https://www.ifrc.org/en/what-we-do/disaster-management/about-disasters/what-is-a-disaster/)  
171 [disaster/](https://www.ifrc.org/en/what-we-do/disaster-management/about-disasters/what-is-a-disaster/)). We are not trying to argue whether “natural disaster” exists or not as this is beyond  
172 the scope of this study. However, the use of this phrase is in line with literature, e.g. Cavallo  
173 and Noy (2011), Smith and Matthews (2015), Ye et al. (2016), Bakkensen et al. (2018).

174 Nevertheless, to avoid any confusion and as we are in general agreement with the reviewer we  
175 **rephrased line 22 to: “ ... lead to an increase of risk to humans and for economic loss**  
176 **potentials from natural hazards e.g., tropical cyclones, with potentially disastrous**  
177 **consequences.” We also checked the whole manuscript and corrected for a more precise**  
178 **use of the terminology in the revised manuscript.**  
179

180  
181

182 *Line 34: you mean “livestock”?*

183  
184

185 We thank Reviewer 1 for pointing this out and the reviewer is correct. **We have corrected**  
186 **this.**

187  
188

189 *Lines 145-149: It is mentioned that VIF is used to resolve the issue of collinearity and 17*  
190 *variables are selected to construct the final LRC model. How many total variables were*  
191 *included initially? Are the VIF values for all of these 17 variables less than the normal*  
192 *threshold (i.e.,  $VIF \leq 7.5$ )? It would be useful to add the VIF values of the final variables in*  
193 *Table 3.*

194  
195

196 The list of variable initially used is presented in Table 2. We have modified the caption of  
197 Table 2 for clarification.

198 Yes, those 17 variables stated in Table 3 have VIF value of less than 5. We are not sure whether  
199 including the VIF values of the final variables would be useful for this manuscript. However,  
200 Reviewer 1 pointed out that we did not state the criteria which we used for the variable selection.

201 **We have included the criteria (i.e.  $VIF < 5$ ) for the variable selection in the manuscript.**

202 **Line 176-177: “Variables with VIF value larger than 5 are excluded.”**

203  
204

205 *Lastly, a thorough intermediate level editing is recommended to remove “several”*  
206 *grammatical and language errors throughout the manuscript.*

207

208 We thank Reviewer 1’s advice, and **we have edited the manuscript accordingly.**

209

## 210 **References**

211 Bakkensen, L. A., Shi, X., and Zurita, B. D.: The Impact of Disaster Data on Estimating  
212 Damage Determinants and Climate Costs, *Economics of Disasters and Climate Change*,  
213 2, 49-71, 10.1007/s41885-017-0018-x, 2018.

214 Befort, D. J., Fischer, M., Leckebusch, G. C., Ulbrich, U., Ganske, A., Rosenhagen, G., and  
215 Heinrich, H.: Identification of storm surge events over the German Bight from  
216 atmospheric reanalysis and climate model data, *Natural Hazards and Earth System*  
217 *Sciences*, 15, 1437, 2015.

218 Befort, D. J., Wild, S., Kruschke, T., Ulbrich, U., and Leckebusch, G. C.: Different long-term  
219 trends of extra-tropical cyclones and windstorms in ERA-20C and NOAA-20CR  
220 reanalyses, *Atmos Sci Lett*, 17, 586-595, 10.1002/asl.694, 2016.

221 Befort, D. J., Wild, S., Knight, J. R., Lockwood, J. F., Thornton, H. E., Hermanson, L., Bett, P.  
222 E., Weisheimer, A., and Leckebusch, G. C.: Seasonal forecast skill for extratropical  
223 cyclones and windstorms, *Q J Roy Meteor Soc*, 145, 92-104, 10.1002/qj.3406, 2019.

224 Befort, D. J., Kruschke, T., and Leckebusch, G. C.: Objective identification of potentially  
225 damaging tropical cyclones over the Western North Pacific, *Environmental Research*  
226 *Communications*, 2, 031005, 10.1088/2515-7620/ab7b35, 2020.

227 Cavallo, E., and Noy, I.: Natural Disasters and the Economy — A Survey, *International Review*  
228 *of Environmental and Resource Economics*, 5, 63-102, 10.1561/101.00000039, 2011.

229 Emanuel, K., Ravela, S., Vivant, E., and Risi, C.: A statistical deterministic approach to  
230 hurricane risk assessment, *B Am Meteorol Soc*, 87, 299-314, 10.1175/Bams-87-3-299,  
231 2006.

232 Kruschke, T.: Winter wind storms: Identification, verification of decadal predictions, and  
233 regionalization, *Doktors der Naturwissenschaften, Institut für Meteorologie, Freie*  
234 *Universität at Berlin*, 181 pp., 2015.

235 Leckebusch, G. C., Renggli, D., and Ulbrich, U.: Development and Application of an Objective  
236 Storm Severity Measure for the Northeast Atlantic Region, *Meteorologische Zeitschrift*,  
237 17, 575-587, 10.1127/0941-2948/2008/0323, 2008.

238 Nissen, K. M., Ulbrich, U., Leckebusch, G. C., and Kuhnel, I.: Decadal windstorm activity in  
239 the North Atlantic-European sector and its relationship to the meridional overturning  
240 circulation in an ensemble of simulations with a coupled climate model, *Climate*  
241 *Dynamics*, 43, 1545-1555, 10.1007/s00382-013-1975-6, 2014.

242 Osinski, R., Lorenz, P., Kruschke, T., Voigt, M., Ulbrich, U., Leckebusch, G. C., Faust, E.,  
243 Hofherr, T., and Majewski, D.: An approach to build an event set of European  
244 windstorms based on ECMWF EPS, *Nat. Hazards Earth Syst. Sci.*, 16, 255-268,  
245 10.5194/nhess-16-255-2016, 2016.

246 Sajjad, M., and Chan, J. C. L.: Risk assessment for the sustainability of coastal communities:  
247 A preliminary study, *Science of The Total Environment*, 671, 339-350,  
248 <https://doi.org/10.1016/j.scitotenv.2019.03.326>, 2019.

249 Sajjad, M., Chan, J. C. L., and Kanwal, S.: Integrating spatial statistics tools for coastal risk  
250 management: A case-study of typhoon risk in mainland China, *Ocean & Coastal*  
251 *Management*, 184, 105018, <https://doi.org/10.1016/j.ocecoaman.2019.105018>, 2020.

252 Smith, A. B., and Matthews, J. L.: Quantifying uncertainty and variable sensitivity within the  
253 US billion-dollar weather and climate disaster cost estimates, *Nat Hazards*, 77, 1829-  
254 1851, 10.1007/s11069-015-1678-x, 2015.

255 Swiss Re: Natural catastrophes and man-made disasters in 2015: Asia suffers substantial losses.  
256 [https://reliefweb.int/sites/reliefweb.int/files/resources/sigma1\\_2016\\_en.pdf](https://reliefweb.int/sites/reliefweb.int/files/resources/sigma1_2016_en.pdf), 2016.

257 Vickery, P. J., Skerlj, P. F., and Twisdale, L. A.: Simulation of Hurricane Risk in the U.S.  
258 Using Empirical Track Model, *Journal of Structural Engineering*, 126, 1222-1237,  
259 10.1061/(ASCE)0733-9445(2000)126:10(1222), 2000.

260 Walz, M. A., and Leckebusch, G. C.: Loss potentials based on an ensemble forecast: How  
261 likely are winter windstorm losses similar to 1990?, *Atmos Sci Lett*, 20, e891,  
262 10.1002/asl.891, 2019.

263 Ye, T., Wang, Y., Wu, B., Shi, P., Wang, M., and Hu, X.: Government Investment in Disaster  
264 Risk Reduction Based on a Probabilistic Risk Model: A Case Study of Typhoon  
265 Disasters in Shenzhen, China, *International Journal of Disaster Risk Science*, 7, 123-  
266 137, 10.1007/s13753-016-0092-7, 2016.

267 **Response to Reviewer 2's comments**

268

269 We thank Reviewer 2 for the time to go through our manuscript in details. This manuscript  
270 describes a new and efficient method to produce a physical TC event set in the western North  
271 Pacific basin. In general, reviewers think after careful revision, the results of this study is of  
272 great interest and relevance, and it will be a useful contribution to the field of TC risk  
273 assessment. Here is our point-to-point response to Reviewer 2's comments. Reviewer 2's  
274 comments are in red.

275

276

277 **General comments:**

278 *This manuscript describes a new and efficient method to produce TC event set in the Pacific*  
279 *basin. The TC events are detected from an ensemble data archive TIGGE, using an objective*  
280 *impact-oriented windstorm identification algorithm WiTRACK. This dataset contributes to*  
281 *existing synthetic datasets (mostly statistical basin-wide methods) as in this dataset the TCs*  
282 *are detected in GCMs, so that the complex physical processes of TCs are captured and hence*  
283 *TCs are physically realistic. More extreme TCs are found in the dataset and these data will*  
284 *help overcome the shortage in observational record. Overall, I think the results will be a nice*  
285 *contribution to the field of TC risk assessment. However, I have some basic questions about*  
286 *the methodology, the utility of certain results and I recommend major revisions prior to*  
287 *publication. Also, I would recommend careful editing of the manuscript. There are many*  
288 *terminologies in the manuscript and please make sure it is easy for readers to follow.*

289

290

291 We thank the reviewer advice and we have carefully reviewed and edited the manuscript.

292

293

294 **Major comments:**

295 *1) L191: The detection rates of historical TCs are reported here. However, will the detection*  
296 *algorithm produce more TCs? What fraction of TCs that the detection algorithm produce is*  
297 *real historical TCs?*

298

299

300 We thank the reviewer for pointing this out and highlighting a section for which we can  
301 improve clarity. Strictly spoken, the detection algorithm we apply in this study (developed for  
302 TC detection in the West-Pacific in Befort et al., 2020) does not produce TCs, but enables us  
303 to detect them automatically in the large data set. As the data set we use is the output of  
304 operational NWP's forecast models, in a very narrow sense , none of the TCs that we detected  
305 is a one-to-one equivalent to a real historical TCs. However, events which satisfy the criteria  
306 in the MPES TC identifier (MTI, Section 3.2.3) (i.e. MEPS TC events) can be considered as  
307 events which are similar to the historical event. The percentage of TCs which are in this sense  
308 similar to real events that occurred in the TIGGE is ~60%. Thus, about 40% are pure ensemble  
309 predicted events that did not realise in the observed nature or do not have a very similar twin  
310 at the same time at the same location.

311

312 **We have modified the text in L191 and the caption of Table 4 for more accurate**  
313 **description. Lines 225-228, "A historical TC is said to be detected in a forecast model if there**  
314 **exists a TC counterpart in the forecast model, which is similar to the historical TC as identified**

315 *by the MTI (Section 3.2.3). The detection rates of historical TCs which are detected in different*  
316 *forecast outputs, i.e. CMA, ECMWF, JMA, and NCEP, are 91.2%, 94.7%, 89.4%, and 90.7%,*  
317 *respectively, ...”*

318  
319

320 *2) The authors mention that one benefit of this dataset is “The TPEPS event set includes events*  
321 *which are unlikely but physically possible. This provides an important and unique advantage*  
322 *for typhoon risk assessment.” Combined with Fig. 2, TC tracks in the detected dataset is very*  
323 *different with observations, and TPEPS tracks appear in locations with no historical tracks. If*  
324 *there is no historical track in some regions, are they supposed to be no storms or there can be*  
325 *storms but no storm has appeared in historical records due to the low probability? This needs*  
326 *to be explained.*

327  
328

329 We thank Reviewer 2 for pointing out this important issue. If there is no historical track in  
330 some regions, this does not mean storms cannot occur in those regions. The fact that we have  
331 not seen a TC during the time period of known observational records in those regions could be  
332 due to the observation period is too short and the sample size is not large enough to fully  
333 represent the distribution of the underlying basic population (i.e. all possible TCs in the given  
334 climate state). For example, if we follow the necessary but insufficient conditions of TC  
335 formation which are identified by Gray (1977) from historical observations, TC formation  
336 occurs away from the equator ( $> 5$  deg). However, Tropical Storm Vamei (2001) formed close  
337 to the equator ( $\sim 1.4$  deg N). This shows storm can appear in the historically “storm-free”  
338 region.

339

340 Furthermore from the statistical perspective, we can view the JRA-55 event set as a subset  
341 which is randomly selected from the TPEPS event set. This means if we randomly sample the  
342 TPEPS event set, we can obtain a subset highly similar to the JRA-55 event set. For  
343 demonstration, we have conducted bootstrap resampling on the TPEPS event set to obtain  
344 10,000 sets of subsample. Each set of subsamples has 668 events to mimic the number of  
345 events in the JRA-55 event set. For each set of subsamples, the track density is calculated, and  
346 used to calculate uncentred pattern correlation between the resampling set of subsamples and  
347 the JRA-55 event set. In order to focus on relevant entries, for a particular grid box, if the  
348 values of track density for a resampling set and the JRA-55 event set are both less than one,  
349 such grid box is not used in the pattern correlation calculation. The mean, standard deviation,  
350 minimum, and maximum of the uncentred pattern correlation of the 10,000 set of subsamples  
351 are 0.9380, 0.0107, 0.8961, and 0.9697, respectively. This suggests the spatial pattern of the  
352 JRA-55 event set is highly similar to a small random subset of the TPEPS event set.  
353 Consequently, the JRA-55 event set can be seen as a subset randomly selected from the TPEPS  
354 event set. On the other hand, it is not be possible to deduce the basic population (e.g. the TPEPS  
355 event set) from a small sample set (e.g. the JRA-55 event set). Although the spatial distribution  
356 of the small set sample is similar to the subsamples of the basic population and thus usable as  
357 one possible realisation of the basic population, the small sample set does not contain all of the  
358 information of the underlying population. Furthermore, the statistical estimate of extremes  
359 would also be different for the small sample set (e.g. JRA-55 event set) and the basic population  
360 (e.g. TPEPS event set).

361 **We have included the above explanation in the revised manuscript (Lines 259-280).**

362  
363



364 *3) The sensitivity and performance of four ensemble data archive are not well described. For*  
365 *example, in some dataset, the storms are much weaker than historical storms. And some models*  
366 *have biases in simulating extratropical cyclone transition. More explanations and descriptions*  
367 *of the data archive needs to be added. Also, how these biases would have an impact on the*  
368 *detection algorithm?*

369  
370 The four data sets selected from the TIGGE archive are the state-of-the-art NWP models as  
371 used by four leading synoptic weather forecast centres worldwide. Although a full assessment  
372 of their respective models' skill and potential biases is not in the scope of this study, **we added**  
373 **a section with information on the general performance of these four selected NWP models**  
374 **(Lines 105-115)**. For the dedicated purpose of this study, the reviewer is fully correct and we  
375 need to check for biases in the underlying climatological features as provided by a time- and  
376 ensemble-aggregated view of the data set (a task normally not necessarily done in forecast  
377 model evaluation departments for all levels of severe and rare extremes). This evaluation for  
378 extreme TC occurrence is what we did in section 4.1, showing respective results in Fig.1-7.  
379 **We included a paragraph to clarify which part of the study is model validation and which**  
380 **part is event set building (Lines 223-225)**.

381  
382 TIGGE data's main difference to the operationally used NWP output is that TIGGE did archive  
383 a lower resolution. Nevertheless, all underlying processes and feedbacks are captured in the  
384 originally resolution of the NWP products and are thus fully included. Thus, we would expect  
385 the best possible representation of dynamical processes in those forecast simulations than  
386 compared to lower resolution AOGCM simulations, e.g. for transient climate experiments.  
387 Beyond this, model resolution is known to be a limiting fact of simulating TC intensity  
388 (Bengtsson et al., 2007). One of the advantages of using WiTRACK is that it does not use raw  
389 wind speeds, instead, it uses the 98<sup>th</sup> percentile relative exceedance for tracking. This means  
390 that even if the simulation wind speed of TC is systematically weaker than in historical  
391 observations, the 98<sup>th</sup> percentile climatological wind should also be lower than the actual 98<sup>th</sup>  
392 percentile climatological wind speed, a TC will still be tracked as long as there exists a 98<sup>th</sup>  
393 percentile exceedance wind cluster. It can be shown that, within the study area, the 98<sup>th</sup>  
394 percentile relative exceedance of the 4 models, which we used to construct the TIGGE event  
395 set, have similar behaviour (i.e. similar to Figure 2 of Osinski et al. (2016)). Befort et al. (2020)  
396 showed the applicability of such an approach to relate information from observations (i.e.  
397 IBTrACS data) to automatically detected TCs from a much coarser resolution reanalysis  
398 product (JRA-55). Consequently, a bias due to resolution does not have significant impact on  
399 WiTRACK as the tracking algorithm serves as a bias correction in this sense (detailed  
400 discussion on the impact of weaker wind speed in model outputs on WiTRACK can be found  
401 in Osinski et al. (2016)). **We included a paragraph to discuss this in more detail (Lines 125-**  
402 **127; 140-152)**.

403  
404  
405 *4) The authors have compared the TIGGE PEPS TCs with JRA-55 in terms of track density,*  
406 *landfall frequency, etc. How about other characteristics? For example, landfall intensity along*  
407 *coastline?*

408  
409  
410 The distribution of landfall intensity (wind speed in m/s) for TC, which made landfall with at  
411 least typhoon strength, are very similar for the JRA-55 event set and TPEPS event set. The  
412 table below shows some of the statistics of these two distributions. The two-sample

413 Kolmogorov-Smirnov test show these two distributions belong to the same distribution  
414 significant at the 0.05 significance level.  
415

	JRA-55	TPEPS
Mean	23.5899	23.4044
Standard deviation	3.44527	3.84537
Median	22.58	22.2
Number of events	184	23343

416  
417 **We have included the above discussion into revised manuscript [Lines 345-348].**  
418

419  
420 *5) Fig. 7 shows the difference between TIGGE PEPS event set and observation. In the text, you*  
421 *have mentioned possible reasons for these differences. Is there possible way to reduce these*  
422 *differences, for example in the detection algorithm, to also remove low-impact storms? Also,*  
423 *you mentioned the ESSI, is there a way to quantify this index?*  
424

425  
426 Figure 7 shows some of the differences between the TPEPS event set and the JRA-55 event set.  
427 These differences are mainly due to the finite simulation time in forecast models. Some of  
428 these differences could be reduced based on additional assumptions that would depend on the  
429 specific application of the users. A more detailed analysis of the performance with respect to a  
430 data set not affected by a finite simulation time is a reanalysis product (e.g. JRA-55). We  
431 showed in Befort et al. (2020) in JRA-55 that our tracking already focusses on the most severe  
432 part of the TC severity distribution and thus does show some expected differences to e.g.  
433 IBTrACS data.  
434

435 We apologise we did not include the text associated with the SSI (and ESSI). Leckebusch et al.  
436 (2008) introduced this objective severity measure for gridded datasets of extreme storms in the  
437 North-Atlantic and the method was applied for TCs in the North-West Pacific in Befort et al.  
438 (2020). **The relevant text is included in revised manuscript [Lines 215-219].**  
439

440  
441 **Minor comments:**

442 *L41-42: more recent papers should be added. Such as the following two recent models:*  
443 *- Lee, C.-Y., M. K. Tippett, A. H. Sobel, and S. J. Camargo, 2018: An environmentally*  
444 *forced tropical cyclone hazard model. Journal of Advances in Modeling Earth Systems,*  
445 *10 (1), 223–241.*  
446 *- Jing, R., and N. Lin, 2020: An environment-dependent probabilistic tropical cyclone*  
447 *model. Journal of Advances in Modeling Earth Systems, 12 (3), e2019MS001 975.*  
448

449  
450 We thank the reviewer's suggestions. **We have included these references in the revised**  
451 **manuscript.**  
452

453  
454 *L45: I didn't understand the sentence 'the typhoon event set might not be physically consistent'.*  
455 *What is 'physically' consistent?*  
456

457 It means event sets created by stochastic perturbations will create TC events that (with respect  
458 to their inner dynamical structure) are not necessarily physically consistent anymore. As just  
459 surface footprints are stochastically modelled from existing tracks, there is no check whether  
460 those events (in the stochastically modelled from) are physically possible and how they could  
461 be realised in a fully dynamical consistent view, thus fulfilling all known physical relations and  
462 derived constraints by the means of physical laws. Consequently, the amount of unrealistic  
463 physical properties due to the oversimplified stochastic simulation is unknown and laws of  
464 physical interactions are potentially ignored. **We have modified the sentence in the revised  
465 manuscript to clarify this point [see lines 45-51].**

466

467 *L179: “The domain of this study covers the Western North Pacific (WNP), east and south-east  
468 Asia spanning from 85 E to 195E and 15 S to 75 N.” Why data around equator is also used?  
469 There is no TCs forming around equator.*

470

471 We thank Reviewer 2 for pointing this out and we apologise for the confusion. The domain  
472 stated in the manuscript is part of the parameter set up for WiTRACK. However, the true  
473 domain which is used for tracking is 90-180° E, and 0-70° N and **we have made this  
474 correction in the revised manuscript.**

475

476 We included regions close to the equator although TCs rarely form around the equator, it is  
477 still possible for TCs to form close to the equator, for example Tropical storm Vamei (2001).  
478 Furthermore, while the core pressure centre of the TCs might be away from the equator, the  
479 damaging wind field, as identified by the 98<sup>th</sup> percentile relative exceedance, could be quite  
480 large, impacting potentially regions close to the equator.

481

482

483 *L102-104: Is there a reason why an old version of IBTrACS is used?*

484

485

486 IBTrACS v03r10 was the most up-to-date official version of IBTrACS when this study was  
487 first started. Furthermore, for our study period (with 6-hourly observations), the data in v04  
488 and v03r10 are the same.

489

490

491 *L152: “the accuracy of the LRC is about 90%” What is the fraction of TC (or positive samples?)  
492 Does there exist issue of imbalanced data?*

493

494

495 No, the validation set is not imbalanced. In the validation set, 49 out of 96 tracks are TCs  
496 (~51% of the validation set). **We have included a more detailed description in the revised  
497 manuscript. Lines 180-181 “Validation using JRA-55 event set (2015-2017), which has 49 TC  
498 events and 47 non-TC events...”**

499

500

501 *L197: “Percentage of total TC windstorms as PEPS TCs can be treated as a proxy to quantify  
502 the forecast skill of the model.” In Table 5, NCEP is almost twice of that in JMA, what does  
503 this percentage mean?*

504

505

506 This indicates the NCEP model generates more “wrong” forecasts than JMA yet these wrong  
507 forecasts are physically possible. **We included a clarifying sentence to a respective possible**  
508 **interpretation at lines 235-238:** “For example, NCEP has 47.1% of TC windstorms as PEPS  
509 TCs whereas JMA has 26.5%. This indicates the NCEP model generates more “wrong”  
510 forecast than JMA however these wrong forecasts are physically possible. Yet, examining the  
511 forecast skill of models is not the focus of this study and the rest of the discussion focuses on  
512 the TPEPS TC event set.”

513  
514

515 *L203: do you mean Fig 3? Also, more explanations should be added in the text. I can't*  
516 *understand this figure.*

517

518 We thank Reviewer 2 for identifying this error. The reviewer is correct that we are referring  
519 to Fig 3. Fig. 3 shows the feature scaled times series of number of TCs which are first identified  
520 in each day from May to December. The core message of Fig 3 is that the temporal variability  
521 of the TPEPS event set and the JRA-55 event set are largely similar (except for the earlier  
522 years). **We have modified the text in the revised manuscript. Lines 239-240** “Figures 2  
523 and 3 show the spatial pattern and temporal variability of the number of TC which are first  
524 detected for each day, ...”

525

526

527 *L203: In Fig. 2, all TPEPS are much more similar with each other, comparing with JRA-55.*  
528 *How to explain this?*

529

530

531 The major difference between the track density of TPEPS and JRA-55 is that there is an  
532 eastward bias in the TPEPS. There are several reasons that could contribute to this. The  
533 eastward bias in the track density appears to be a common feature in many GCMs (e.g.  
534 Camargo et al., 2005; Bell et al., 2013; Roberts et al., 2020), this has also been observed in  
535 seasonal forecast output (Camp et al., 2015). Finite simulation time has also contributed to this  
536 bias as TC that forms in the region east of 150 °E would not have the time to move into the  
537 western part of WNP before the end of simulation time. Differences in the amount of tracks  
538 could also contribute to the differences as more diverse tracks would be captured. **We have**  
539 **added a respective explanatory comment at lines 252-258.**

540

541

542 *Fig4: The tracks in black are very easily messed up with the map. Probably change the color*  
543 *of coastline.*

544

545

546 We thank Reviewer 2 for pointing this out. **We have changed the colour of the plot.**

547

548

549 *Fig5: The y-axis is not clear to me, please add more explanation.*

550

551 Fig 5 shows the climatological seasonal cycle of TC activity for the TPEPS TC event set and  
552 the JRA-55 event set. The daily number distribution,  $p_i$ , is calculated as follows:

553

554  
555  
556  
557  
558  
559  
560  
561  
562  
563  
564  
565  
566  
567  
568  
569  
570  
571  
572  
573  
574  
575  
576  
577  
578  
579  
580  
581  
582  
583  
584  
585  
586  
587  
588  
589  
590  
591  
592  
593  
594  
595  
596  
597  
598  
599  
600  
601

$$p_i = \frac{n_i}{\sum_i n_i} \times 100\%$$

where  $n_i$  is the number of TC first detected on day  $i$  for the individual event set. As such, it is the probability of TC being first detected at a given day. **We have added more explanation in the caption of Figure 5.**

*Fig8: The colored dots for single center are too light to see. If this figure is to show distribution, I would recommend not using same color bar for single model and for TIGGE total.*

**We have changed the colour scale of this figure in the revised manuscript.**

*Fig9: It's hard to see the distributions are in good agreement, probably can change to annual frequency instead of total number of landfall events. Also, the correlation coefficients could be used to show the landfall frequency in all TIGGE dataset is positively correlated with JRA-55.*

We thank Reviewer 2 for these suggestions. **We have included pattern correlation between the spatial distribution for JRA-55 and TPEPS event sets in the revised manuscript. Line 339 "...with uncentred pattern correlation of 0.8345."**

*Fig12: I can see your points in showing the grey dashed lines. But the lower bound curves cannot show the trend properly. I would recommend add 75% or 80% confidence interval to show that the trends are same, but TIGGE PEPS event set has much narrower bounds.*

We are not certain what Reviewer 2 refers to as the trend of the lower bound curves. There are two separate factors that determine the "shape" of the curve of the lower and upper bound of uncertainty. First, the return level-return period estimate has asymptotic behaviour. This means the return level estimate approaches to a certain value as the return period increases. Second, the uncertainty of the estimation increases with increasing return period. Combining these two factors we can see that the so-called "trend" in the lower bound grey curve does not exist. To show the 95% confidence interval reflects a typical setting for assessing statistical estimates uncertainty for GPD fitted return-level plots and the authors would prefer to stay with this representation.

## **References**

- Bell, R., Strachan, J., Vidale, P. L., Hodges, K., and Roberts, M.: Response of Tropical Cyclones to Idealized Climate Change Experiments in a Global High-Resolution Coupled General Circulation Model, *J Climate*, 26, 7966-7980, 10.1175/JCLI-D-12-00749.1, 2013.
- Bengtsson, L., Hodges, K. I., and Esch, M.: Tropical cyclones in a T159 resolution global climate model: Comparison with observations and re-analyses, *Tellus A*, 59, 396-416, 2007.

- 602 Camargo, S. J., Barnston, A. G., and Zebiak, S. E.: A statistical assessment of tropical cyclone  
603 activity in atmospheric general circulation models, *Tellus A*, 57, 589-604,  
604 10.1111/j.1600-0870.2005.00117.x, 2005.
- 605 Camp, J., Roberts, M., MacLachlan, C., Wallace, E., Hermanson, L., Brookshaw, A., Arribas,  
606 A., and Scaife, A. A.: Seasonal forecasting of tropical storms using the Met Office  
607 GloSea5 seasonal forecast system, *Q J Roy Meteor Soc*, 141, 2206-2219,  
608 10.1002/qj.2516, 2015.
- 609 Gray, W. M.: Tropical Cyclone Genesis in the Western North Pacific, *J Meteorol Soc Jpn*, 55,  
610 465-482, 1977.
- 611 Osinski, R., Lorenz, P., Kruschke, T., Voigt, M., Ulbrich, U., Leckebusch, G. C., Faust, E.,  
612 Hofherr, T., and Majewski, D.: An approach to build an event set of European  
613 windstorms based on ECMWF EPS, *Nat. Hazards Earth Syst. Sci.*, 16, 255-268,  
614 10.5194/nhess-16-255-2016, 2016.
- 615 Roberts, M. J., Camp, J., Seddon, J., Vidale, P. L., Hodges, K., Vanniere, B., Mecking, J.,  
616 Haarsma, R., Bellucci, A., Scoccimarro, E., Caron, L.-P., Chauvin, F., Terray, L.,  
617 Valcke, S., Moine, M.-P., Putrasahan, D., Roberts, C., Senan, R., Zarzycki, C., and  
618 Ullrich, P.: Impact of Model Resolution on Tropical Cyclone Simulation Using the  
619 HighResMIP-PRIMAVERA Multimodel Ensemble, *J Climate*, 33, 2557-2583,  
620 10.1175/JCLI-D-19-0639.1, 2020.

621

622

623 **Response to Reviewer 3's comments**

624

625 We thank Reviewer 3 for the time to go through our manuscript in details. This manuscript  
626 describes a new and efficient method to produce a physical TC event set in the western North  
627 Pacific basin. In general, reviewers think after careful revision, the results of this study is of  
628 great interest and relevance, and it will be a nice contribution to the field of TC risk assessment.  
629 Here is our point-to-point response to Reviewer 3's comments. Reviewer 3's comments are in  
630 red.

631

632 **General Comment**

633 *I think that the topic of this study is of great interest and relevance, and that it is suitable to*  
634 *NHESS. Besides, the paper is generally well written, the methodology clearly illustrated and*  
635 *the results well presented and discussed. However, there are also a few (minor) corrections*  
636 *and some improvements of the text that could be made to further improve the manuscript before*  
637 *to proceed with its publication.*

638

639 *Therefore, my recommendation is to accept the manuscript for publication after **minor***  
640 *revisions.*

641

642

643 **Specific Remarks**

644 1. Page 1, line 14: "... characteristics of the new event set is consistent to the..." should read  
645 "... characteristics of the new event set are consistent to the..."

646

647

648 We thank Reviewer 3 for pointing this out, **we have corrected this in the revised manuscript.**

649

650

651 2. Page 1, line 24: "... 67.1 billion RMB ..." Many readers could be helped to understand the  
652 economic significance of this figure by accompanying it with the corresponding value in  
653 US Dollars or Euros.

654

655 We thank Reviewer 3's suggestion, **we have added the corresponding value in Euros in the**  
656 **revised manuscript.**

657

658 3. Page 2, line 45: "... (ii) the storms in the typhoon event set might not be physically  
659 consistent." Please, clarify what do you exactly mean here with "physically consistent"?

660

661 It means event sets created by stochastic perturbations will create TC events that (with respect  
662 to their inner dynamical structure) are not necessarily physically consistent anymore. As just  
663 surface footprints are stochastically modelled from existing tracks, there is no check whether  
664 those events (in the stochastically modelled from) are physically possible and how they could  
665 be realised in a fully dynamical consistent view, thus fulfilling all known physical relations and  
666 derived constraints by the means of physical laws. Consequently, the amount of unrealistic  
667 physical properties due to the oversimplified stochastic simulation is unknown and laws of

668 physical interactions are potentially ignored. **We have modified the sentence in the revised**  
669 **manuscript to clarify this point [see lines 45-51].**

670

671

672

673 4. *Page 2, line 63–64: “In this study, we show the TPEPS event set has much higher*  
674 *information content: more TC events and more extremely high impact TC events.” Higher*  
675 *and more than what?*

676

677

678 We thank Reviewer 3 for pointing out this point. **This sentence should read “In this study,**  
679 **we show the TPEPS event set has much higher information content: more TC events and**  
680 **more extremely high impact TC events than historical or reanalysis-based TC event set.”**  
681 **(Lines 69-70)**

682

683

684 5. *Page 4. Line 126: “WiTRACK identifies windstorm events of all kind, including MEPS TCs,*  
685 *PEPS TCs, MEPS extratropical cyclones.” I suppose it identifies also PEPS extratropical*  
686 *cyclones.*

687

688 Yes, it does. **We have added PEPS extratropical cyclones to the list for clarification.**

689

690

691 6. *Page 4, line 175: “The removal of these events ensures the TPEPS event set is independent*  
692 *of any pre-existing weather patterns.” The goal here is to build a large set of typhoon*  
693 *events in order to provide a solid statistical evaluation of their characteristics, so why is it*  
694 *so important that the considered TPEPS events are independent of any pre-existing weather*  
695 *patterns?*

696

697

698 To use this as an extension of event numbers and thus as an alternative reality, the inclusion of  
699 real existing events will incorporate some bias towards observed events as all of them will  
700 create a multiple realisation in the ensemble members started at the time such a real event  
701 occurred. By not considering those ensemble members, which are closely related to observed  
702 events, will secure that indeed new events are used to build the pure EPS event set. It has to be  
703 noted though that the inclusion of those events should not change the overall track distribution,  
704 or in other words, the track distribution from pure EPS and real EPS events is fairly similar.

705

706

707 7. *Page 6, line 193, Figure 1: please add the units to the colour bar.*

708

709

710 **We have added the unit to colour bar.**

711

712

713 8. *Page 6, line 197, Table 5: Why there is such a large difference in the number of simulated*  
714 *TC wind storms between the TIGGE models? Is this due to the different number of ensemble*  
715 *members of the EPSs? The large majority of the considered TPEPS are from two EPSs: the*  
716 *ECMWF and the NCEP. What consequences could this fact have on the analysis results?*



717  
718  
719  
720  
721  
722  
723  
724  
725  
726  
727  
728  
729  
730  
731  
732  
733  
734  
735  
736  
737  
738  
739  
740  
741  
742  
743  
744  
745  
746  
747  
748  
749  
750  
751  
752  
753  
754  
755  
756  
757  
758  
759  
760  
761  
762  
763  
764

The main reasons for differences in the number of detected TC windstorms between TIGGE models are they have (1) different numbers of ensemble members of the EPSs, (2) different number of runs per day, and (3) different maximum forecast lead time (c.f. Table 1). Given the spatial and temporal distributions of the individual PEPS event sets are similar to each other, the analysis on the overall TPEPS event set is reliable.

9. *Page 6, line 202: Fig. 1d, should read Fig. 2d.*

We thank Reviewer 3 for pointing this out, **we have corrected this in the revised manuscript.**

10. *Page 6, line 203: Fig. 2 should read Fig. 3.*

We thank Reviewer 3 for pointing this out, **we have corrected this in the revised manuscript.**

*11. Page 6–7, line 212–220: I’m not sure I fully understand the explanation the authors provide for the discrepancy between the spatial distribution of the TPEPS event set and JRA-55 events as shown in Figure 2 (panels c and f). The fact that the JRA-55 event set can be considered as a subset of the TIGGE event set does not explain the difference in spatial distribution. According to this view, in fact, the JRA-55 events can be seen as randomly selected from a larger set (the TIGGE set), and thus they should also be spatially distributed as this event set. Also, why the higher level of the 98th percentile values of the JRA-55 wind should explain the lower number of typhoons in this area?*

We agree with Reviewer 3 that the JRA-55 event set can be seen as a subset randomly selected from a larger set (i.e. the TIGGE event set). This means if we randomly sample the TPEPS event set, we can obtain a subset highly similar to the JRA-55 event set. For demonstration, we have conducted bootstrap resampling on the TPEPS event set to obtain 10,000 sets of subsample. Each set of subsamples has 668 events to mimic the number of events in the JRA-55 event set. For each set of subsamples, the track density is calculated, and used to calculate uncentred pattern correlation between the resampling set of subsamples and the JRA-55 event set. In order to focus on relevant entries, for a particular grid box, if the values of track density for a resampling set and the JRA-55 event set are both less than one, such grid box is not used in the pattern correlation calculation. The mean, standard deviation, minimum, and maximum of the uncentred pattern correlation of the 10,000 set of subsamples are 0.9380, 0.0107, 0.8961, and 0.9697, respectively. This suggests the spatial pattern of the JRA-55 event set is highly similar to a small random subset of the TPEPS event set. Consequently, the JRA-55 event set can be seen as a subset randomly selected from the TPEPS event set. On the other hand, it is **not** be possible to deduce the basic population (e.g. the TPEPS event set) from a small sample set (e.g. the JRA-55 event set). Although the spatial distribution of the small set sample is

765 similar to the subsamples of the basic population and thus usable as one possible realisation of  
766 the basic population, the small sample set does not contain all of the information of the  
767 underlying population. Furthermore, the statistical estimate of extremes would also be  
768 different for the small sample set (e.g. JRA-55 event set) and the basic population (e.g. TPEPS  
769 event set). **We have included the above explanation in the revised manuscript (Lines 259-  
770 280).**

771  
772 Upon further investigation, we found that the 98<sup>th</sup> percentile is not the reason that leads to the  
773 differences in spatial distribution. The major difference between the track density of TPEPS  
774 and JRA-55 is that there is an eastward bias in the TPEPS. There are several reasons that could  
775 contribute to this. The eastward bias in the track density appears to be a common feature in  
776 many GCMs (e.g. Camargo et al., 2005; Bell et al., 2013; Roberts et al., 2020), this has also  
777 been observed in seasonal forecast output (Camp et al., 2015). Finite simulation time has also  
778 contributed to this bias as TC that forms in the region east of 150 °E would not have the time  
779 to move into the western part of WNP before the end of simulation time. Differences in the  
780 amount of tracks could also contribute to the differences as more diverse tracks would be  
781 captured. **We have added a respective explanatory comment at lines 252-258.**

782  
783  
784

785 *12. Page 7, line 248–249: As formulated here, this sentence seems to imply that TCs with  
786 weaker winds are also less spatially extended, which is not true.*

787  
788  
789 The impact area of a TC in this study refers to the total area which has experienced TC-  
790 associated extreme wind (i.e. larger than local climatological 98<sup>th</sup> percentile wind speed).  
791 Given the fact that the wind speed of TC wind field decays radially outward, TC with weaker  
792 winds would have a smaller impact area because the outer wind speed would be below the 98<sup>th</sup>  
793 local climatological wind percentile value. **We have added more descriptions about impact  
794 area in the revised manuscript to clarify this point [Lines 306-307].**

795  
796  
797

798 *13. Page 7, 252–255: “... impact (Befort et al., 2020). Many of the low impact TCs ...” should  
799 probably read “... impact (Befort et al., 2020), many of the low impact TCs ...”.*

800  
801

802 We thank Reviewer 3 for pointing this out, **we have corrected this in the revised manuscript.**

803

804

805 *14. Figure 8: In the text of the manuscript, there are references to panels labelled with letters  
806 (a, b, ... f), but the panels in Figure 8 are not labelled.*

807  
808

809 We thank Reviewer 3 for spotting this error. **We have corrected this in the revised  
810 manuscript.**

811  
812

813 *15. Page 9, line 317: "... based on minimisation of the root-mean-square-error (RMSE) of ...".*  
814 *Of what?*

815  
816 We thank Reviewer 3 for pointing this out, **we have corrected this in the revised manuscript.**  
817 This is the root-mean-square-error of the quantile mapping output.

818  
819

## 820 **References**

821 Bell, R., Strachan, J., Vidale, P. L., Hodges, K., and Roberts, M.: Response of Tropical  
822 Cyclones to Idealized Climate Change Experiments in a Global High-Resolution  
823 Coupled General Circulation Model, *J Climate*, 26, 7966-7980, 10.1175/JCLI-D-12-  
824 00749.1, 2013.

825 Camargo, S. J., Barnston, A. G., and Zebiak, S. E.: A statistical assessment of tropical  
826 cyclone activity in atmospheric general circulation models, *Tellus A*, 57, 589-604,  
827 10.1111/j.1600-0870.2005.00117.x, 2005.

828 Camp, J., Roberts, M., MacLachlan, C., Wallace, E., Hermanson, L., Brookshaw, A., Arribas,  
829 A., and Scaife, A. A.: Seasonal forecasting of tropical storms using the Met Office  
830 GloSea5 seasonal forecast system, *Q J Roy Meteor Soc*, 141, 2206-2219,  
831 10.1002/qj.2516, 2015.

832 Roberts, M. J., Camp, J., Seddon, J., Vidale, P. L., Hodges, K., Vanniere, B., Mecking, J.,  
833 Haarsma, R., Bellucci, A., Scoccimarro, E., Caron, L.-P., Chauvin, F., Terray, L.,  
834 Valcke, S., Moine, M.-P., Putrasahan, D., Roberts, C., Senan, R., Zarzycki, C., and  
835 Ullrich, P.: Impact of Model Resolution on Tropical Cyclone Simulation Using the  
836 HighResMIP-PRIMAVERA Multimodel Ensemble, *J Climate*, 33, 2557-2583,  
837 10.1175/JCLI-D-19-0639.1, 2020.

838

839

840

# A New View on Risk of Typhoon Occurrence in the Western North Pacific

Kelvin. S. Ng<sup>1</sup>, Gregor. C. Leckebusch<sup>1</sup>

<sup>1</sup>School of Geography, Earth and Environmental Sciences, University of Birmingham, Birmingham, UK

Correspondence to: Kelvin S. Ng (k.s.ng@bham.ac.uk)

**Abstract.** To study high impact tropical cyclone (TC) is of crucial importance due to its extraordinary destruction potential that leads to major losses in many coastal areas in the Western North Pacific (WNP). Nevertheless, because of the rarity of high-impact TCs, it is difficult to construct a robust ~~hazard~~**risk** assessment based on the historical best track records. **This paper aims to address this issue by introducing a computationally simple and efficient approach to build a physically consistent, high impact TC event set with non-realised TC events in the THORPEX Interactive Grand Global Ensemble (TIGGE) archive. This event set contains more than 10,000 years of TC events.** ~~using data from the THORPEX Interactive Grand Global Ensemble (TIGGE) archive with the application of impact oriented tracking algorithm, to build a physically consistent high impact typhoon event set with non-realised TC events—data equivalent to more than 10,000 years of TC events.~~ The temporal and spatial characteristics of the new event set **are** consistent to the historical TC climatology in the WNP. It is shown that this TC event set contains ~100 and ~77 times more Very Severe Typhoons and Violent Typhoons than the historical records, respectively. Furthermore, this approach can be used to improve the return period estimation of TC-associated extreme wind. Consequently, a robust extreme TC hazard ~~risk~~**assessment**, reflective of the current long-term climate variability phase, can be achieved using this approach.

## 1 Introduction

Increasing frequency and intensity of extreme meteorological events in the recent decades (IPCC, 2012) and increasing number of human population and assets located in risk-prone regions (Desai et al., 2015) lead to an increase of risk **to humans** and **economic** loss potentials ~~to human and economic~~ from natural **hazards** ~~disasters,~~ ~~for example e.g.,~~ tropical cyclones, **with potentially disastrous consequences.** ~~For example, in the period of~~ ~~between~~ 1<sup>st</sup> January and 18<sup>th</sup> October 2018, **total** typhoon-related ~~total~~ direct economic losses in **Western North Pacific (WNP)China** is **evaluated to exceed more than up to 67.4 billion RMB (roughly 8.3 billion Euros)** (Chinese Meteorological Administration, CMA, 2018). While natural ~~disaster hazards~~ ~~has~~ impact ~~to~~ ~~on~~ all **society** stakeholders ~~of the society~~, governments are crucial in disaster risk reduction (DRR) because of their ability to implement necessary DRR-related policy and ability to allocate resources to appropriate parties (Shi, 2012). Governments have various options for DRR investments, for example, post-disaster relief and risk financing. Using cost-benefit analysis for a case study of typhoon disasters in China, Ye et al. (2016) showed insurance premium subsidies has the highest benefit-cost ratio. This is because premium subsidies increases penetration rate of an insurance program, i.e. more protection is offered by the private sector and the risk is transferred to the private sector (Glauber, 2004). Thus, development and application of effective financial instruments for risk transfer is important.

37 Other than classical (re-)insurance solutions, parametric insurance solutions have been developed for test  
38 cases in areas of corn yield (Sun et al., 2014) and **livefe-stock** (Ye et al., 2017) for Southeast Asia and China in  
39 recent years. Swiss Reinsurance Company Ltd. (Swiss Re) insured several municipal governments in Guangdong  
40 Province, China, through parametric insurance solution (Lemcke, 2017). Parametric insurance requires no  
41 physical damage assessment after an event. As soon as a certain threshold (i.e. trigger point) is exceeded, the  
42 insured party receives the agreed compensation from the insurer. Thus it has low administrative cost and quick  
43 disbursement. However, it is a challenge to determine a robust trigger point. It is because it would require a  
44 reliable typhoon **hazard+risk** assessment for the region of interest. A current common approach is to generate a  
45 large typhoon event set (e.g. equivalent to 7,000 years of real world data) based on historical track data using  
46 stochastic approach (e.g. Vickery et al., 2000; Emanuel, 2006; Emanuel et al., 2006; Rumpf et al., 2007, 2009; Lee  
47 et al., 2018; Jing and Lin, 2020). There are two potential downsides with the stochastic approach: (i) such typhoon  
48 event set would be biased toward the past events, and the frequency-intensity distribution of the event set might  
49 not be the same as the underlying frequency-intensity distribution, and; (ii) the storms in the typhoon event set  
50 which are created by stochastic approach are not necessarily physically consistent. As just surface footprints are  
51 stochastically modelled from existing tracks, there is no check whether those stochastically modelled events are  
52 physically possible and how they could be realised in a fully dynamical consistent view, i.e. fulfilling all known  
53 physical relations and derived constraints by the means of physical laws. Consequently, the amount of unrealistic  
54 physical properties due to the oversimplified stochastic simulation is unknown and laws of physical interactions  
55 are potentially ignored.

56 ~~might not be physically consistent (i.e. with unrealistic physical properties) because they are generated~~  
57 ~~using oversimplified models and complex physical interactions are potentially ignored.~~ Consequently, the trigger  
58 point derived from the common approach may not be optimal. This means insurees could be either over- or under-  
59 compensated by the insurer.

60 A method to increase number of extreme weather events is to make use of ensemble prediction system  
61 (EPS). Osinski et al. (2016) used European Centre for Medium-Range Weather Forecasts (ECMWF) EPS to build  
62 an event set of European windstorms. Osinski et al. (2016) pointed out there are two types of storm events  
63 produced by EPS: (i) modified EPS storm (MEPS), and (ii) pure EPS storm (PEPS). MEPSs are storms with  
64 modifications in the EPS which have real-world counterpart. PEPSs are storms in the EPS which have no real-  
65 world counterpart, i.e. unrealised. PEPSs are independent events and the number of PEPSs increases as the lead  
66 time increase until the model has no memory of the initial conditions. Thus one can form an event set of extreme  
67 weather event by using TC related PEPSs. Osinski et al. (2016) demonstrated that reliable statistics of storms  
68 under the observed climate conditions can be produced based on EPS forecasts.

69 Building upon the results of Osinski et al. (2016), a new approach to construct a large data volume,  
70 physically consistent TC event set is presented in this study. This event set is constructed by applying an impact-  
71 oriented windstorm tracking algorithm (WiTRACK; e.g. Leckebusch et al., 2008) (~~WiTRACK; e.g. Leckebusch~~  
72 ~~et al. 2008~~) to a multi-model global operational ensemble forecast data archive, ~~t~~The THORPEX Interactive Grand  
73 Global Ensemble (TIGGE) (Bougeault et al., 2010; Swinbank et al., 2015). The data volume of TIGGE is about  
74 40,000 to 50,000 years. The event set consists of all non-realised TC events which were forecasted by EPS of  
75 different centres, this event set is referred to as the TIGGE PEPS (TPEPS) event set. In this study, we show the

76 TPEPS event set has much higher information content: more TC events and more extremely high impact TC  
77 events ~~than historical or reanalysis-based TC event set~~. The TPEPS event set can be used to produce a robust TC  
78 ~~hazard~~ risk assessment and to determine a robust trigger point for parametric typhoon insurance.

79 In this paper, we first present a computationally simple, inexpensive and efficient method to construct a  
80 physically consistent, high information content TC event set using only the 6-hourly surface wind speed field of  
81 EPS forecast model outputs. Then we analyse the characteristics of the TPEPS event set. Validation of the new  
82 method is done by comparing with the event set which is constructed using reanalysis data. The added values of  
83 this new approach are also discussed and presented. The paper is organised as follows: data sets which are used  
84 in this study are described in Section 2. Section 3 outlined the method that has been used to construct the TPEPS  
85 event set. Results and discussions including validation and investigate the characteristic of the TPEPS event set  
86 are presented in Section 4. A summary and conclusions can be found in Section 5.

## 88 2 Data

89 6-hourly instantaneous 10-m wind speed data in different data archives mentioned below are used in this study  
90 because it is highly related to TC wind damages. The domain of this study covers the Western North Pacific  
91 (WNP), east and south-east Asia spanning from ~~9085° E to 180+95° E and 045° NS to 705° N~~. The Japanese 55-  
92 year Reanalysis (JRA-55) (Kobayashi et al., 2015) from 1979 until 2017 (resolution of  $1.25^\circ \times 1.25^\circ$ ) is used for  
93 validation of the TPEPS event set. JRA-55 (1979-2014) is also used in parameter selection in TC identification  
94 algorithm, construction of Logistic Regression Classifier (LRC) (Sect. 3.2.2), and the data in 2015-2017 ~~are~~  
95 used for validation of LRC. ERA-Interim (ERA-I) (Dee et al., 2011) is also used in the construction of LRC.

96 The TIGGE data archive (Bougeault et al., 2010; Swinbank et al., 2015) is used in the construction of  
97 the PEPS TC event set. The TIGGE data archive has been used extensively in the study of TC activity forecast  
98 (e.g. Vitart et al., 2012; Belanger et al., 2012; Halperin et al., 2013; Majumdar and Torn, 2014; Leonardo and  
99 Colle, 2017; Luitel et al., 2018). ~~TIGGE data archive consists of ~8-15-day ensemble forecast data from 10~~  
100 numerical weather prediction centres with about 11-50 members each. In this study, only perturbed forecast  
101 outputs of EPS from selected centres are used and they are ~~Chinese Meteorological Administration (CMA),~~  
102 ~~European Centre for Medium Range Weather Forecasts (ECMWF),~~ Japanese Meteorological Agency (JMA), and  
103 ~~National Centers for Environmental Prediction (National Centers for Environmental Prediction (NCEP))~~ (cf.  
104 Table 1). ~~These four data sets are chosen because they are the state-of-the-art NWP models, which is used by~~  
105 ~~four leading synoptic weather forecast centres, and they are the most complete dataset in the archive for the study~~  
106 ~~period 2008-2017~~. Model configurations and model updates are documented online at  
107 <https://confluence.ecmwf.int/display/TIGGE/Models>. ECMWF EPS is a variable resolution EPS, i.e. days 1-10  
108 were run at a higher resolution than days 11-15. For computational efficiency, ECMWF EPS outputs are regridded  
109 into a lower resolution grid of  $0.5625^\circ \times 0.5625^\circ$ . The resolution of the selected data sets ranges from  
110  $0.5625^\circ \times 0.5625^\circ$  to  $1.25^\circ \times 1.25^\circ$ . Forecast lead time of each forecast outputs ranges from 216 to 384 hours. Only  
111 forecast outputs, which are initialised during the main typhoon season, i.e. 15 May-30 November, are considered.  
112 The resultant TPEPS TC event set has data equivalent to more than 10,000 years of TC model data of the current  
113 climate state.

114 Many studies have evaluated the performance of these EPSs in forecasting TC activities in various ocean  
115 basins. In general, EPSs underestimate TC intensity especially for coarse resolution models (Hamill et al.,  
116 2010; Magnusson et al., 2014). TC track and genesis forecast error exists in EPS and these errors increase as lead  
117 time increases (Buckingham et al., 2010; Yamaguchi et al., 2015; Zhang et al., 2015; Xu et al., 2016). While  
118 ECMWF EPS forecast would occasionally have abnormal TC track forecast errors (i.e. track forecast error that is  
119 extremely large) and might struggled with developing a warm core in the short range forecast (Majumdar and  
120 Torn, 2014; Xu et al., 2016). ECMWF EPS appears to have better performance in TC track forecast than other  
121 EPSs (Yamaguchi et al., 2015; Zhang et al., 2015; Xu et al., 2016). Yet, a full assessment of the respective skill  
122 in models is not in the scope of this study. For the dedicated purpose of this study, an examination for biases in  
123 the underlying climatological features as provided by a time- and ensemble-aggregated view of the data set is  
124 presented in Sect. 4.1.

125 The International Best Track Archive for Climate Stewardship (IBTrACS) v03r10 (Knapp et al., 2010)  
126 is used for validation and identification of TC events in reanalysis and TIGGE data archive. It contains all of the  
127 available best track records from different centres around the globe up to year 2017. Since only part of the best  
128 track records of year 2017 are archived in this version of IBTrACS, best track data from Joint Typhoon Warning  
129 Centre (JTWC) is used for year 2017.

### 131 3 Methods

#### 132 3.1 Identification and characterisation of ~~TC~~typhoon-related windstorms

133 For identification and characterisation of ~~typhoon~~TC-related windstorms, an impact-oriented tracking algorithm  
134 is used – WiTRACK (Leckebusch et al., 2008; Kruschke, 2015). Befort et al. (2020)- adapted the algorithm to  
135 TCtropical cyclones and showed WiTRACK is well capable to identify high impact TCtyphoon events in WNP,  
136 using coarse resolution reanalysis product, with comparable quality to more data intensive algorithms. A brief  
137 description of the general procedure to track a windstorm using WiTRACK is as follows: (i) clusters with wind  
138 speed above the local threshold are identified for each of the 6-hourly time step of the input dataset; (ii) clusters  
139 with size smaller than a predefined threshold (*minarea*) are excluded; (iii) clusters identified in each 6-hourly  
140 time step are connected to a track using a nearest-neighbour criterion with consideration of the size of the cluster,  
141 and; (iv) events with lifetime less than 8 6-hourly time steps are removed. Majority of the settings of WiTRACK  
142 are identical to Befort et al. (2020), including the use of local 98<sup>th</sup> percentile wind speed as local wind threshold,  
143 except in this study *minarea* is chosen to be 15,000 km<sup>2</sup>. The 98<sup>th</sup> percentile wind speed is chosen because over  
144 90% of loss events with losses above 3,000 million RMB can be identified by WiTRACK as demonstrated by  
145 Befort et al. (2020). The value for *minarea* is chosen based on a series of sensitivity studies for parameter selection.  
146 The output of WiTRACK contains information about the characteristics of all identified windstorm events,  
147 including size of the windstorm at any given 6-hourly time step, the overall footprint of extreme wind associated  
148 with the windstorm events, and storm severity index (SSI; Leckebusch et al., 2008). These information are used  
149 in the identification of ~~TC~~typhoon-related pure EPS windstorm events (Sect. 3.2). As discussed in Sect. 2, TC  
150 intensity is generally underestimated by EPS and model resolution is known to be a limiting factor (Bengtsson et  
151 al., 2007; Hamill et al., 2010; Magnusson et al., 2014). One of the advantages of using WiTRACK is that it does

not use raw wind speeds, instead, it uses 98<sup>th</sup> percentile relative exceedance for tracking. This means that even if the simulation wind speed of TC is systematically weaker than historical observations, the 98<sup>th</sup> percentile climatological wind in the models should also be lower than the observed 98<sup>th</sup> percentile climatological wind. A TC will still be tracked by WiTRACK as long as there exists a 98<sup>th</sup> percentile exceedance wind cluster. Consequently, a bias due to resolution does not have significant impact on WiTRACK as the tracking algorithm serves as a bias correction in this sense (detailed discussion on the impact of weaker wind speed in model outputs on WiTRACK can be found in Osinski et al. (2016)). Furthermore, it can be shown that, within the study area, the 98<sup>th</sup> percentile relative exceedance of the 4 models, which we used to construct the TPEPS TC event set, have similar behaviour (i.e. similar to Figure 2 of Osinski et al. (2016)). Consequently, individual PEPS TC event set can be combined to form a large PEPS TC event set, i.e. TPEPS TC event set.

### 3.2 Identifying ~~TC~~typhoon-related pure EPS windstorm events

WiTRACK identifies windstorm events of all kind, including MEPS TCs, PEPS TCs, MEPS extratropical cyclones, ~~and PEPS extratropical cyclones~~. Therefore additional requirements are needed to identify typhoon-related PEPS TC events. ~~4~~Four post-processing procedures are used: (i) Geographic Filter (GF), (ii) Logistic Regression Classifier (LRC), (iii) MEPS TC Identifier (MTI), and (iv) Detection at Initialisation Filter (DIF).

#### 3.2.1 Geographic Filter (GF)

GF was first introduced by Befort et al. (2020). It aims to remove non-TC-related windstorms, e.g. extratropical cyclones, cold surge outbreaks during the winter monsoon, and equatorial disturbances, from the event set by excluding windstorm events which solely identified north of 26° N and east of 100° E, and latitudinal position exclusively south of 10° N. Befort et al. (2020) found this filter can reduce the false alarm rate (i.e. the ratio between number of identified non-TC related windstorms and total number of detected windstorms) of TC identification in JRA-55.

#### 3.2.2 Logistic Regression Classifier (LRC)

In order to reduce computational cost and increase computational efficiency, the classical methods to determine whether the atmospheric disturbance is a TC or non-TC via cold/warm core determination (e.g. Hart, 2003; Strachan et al., 2013) are not used because these methods require multiple variable fields which increase computational cost significantly. Instead, a statistical learning approach, logistic regression classifier (LRC), is used to determine whether the windstorm event is related to a TC or not. Details and background information of LRC can be found in Hastie et al. (2009) and the *caret* package in R is used for LRC training (Kuhn et al., 2018; available online at <https://github.com/topepo/caret>). LRC is trained using the track characteristics of the event in the JRA-55 and ERA-Interim event set (1979-2014) as explanatory variables (Table 2). This combination of training set is chosen based on preliminary studies of constructing an optimal classifier using different combination of training set. In order to avoid issues that are associated with collinearity, a stepwise Variance Inflation Factor (VIF) selection method is used to identify independent variables. Variables with VIF value larger than 5 are excluded. 17 variables have been chosen to use in the construction of LRC (Table 3). Variables that relate to changes in storm position, lifetime of a storm, and mean wind field structure appear to be the most important variables in the LRC. This is expected as the typical trajectory, duration, and structure of TCs and other



189 windstorms are very different. Validation using JRA-55 event set (2015-2017), which has 49 TC events and 47  
 190 non-TC events, have shown that the accuracy of the LRC is about 90% with low rate of false positives and false  
 191 negatives.

### 192 3.2.3 MEPS TC Identifier (MTI)

193 Since there are many replicated events of forecasted historical TCs (i.e. MEPS) in the operational forecast archive,  
 194 it is necessary to remove these events from our event set to avoid biases toward historical events. Instead of using  
 195 the criteria suggested by Osinski et al. (2016), a set of strict criteria (MTI) is used in this study. This can ensure  
 196 the statistics and climatology of TPEPS event set is not biased toward the historical events. The MTI eliminates  
 197 forecast of MPES TC events where the forecasts of those MPES TCs were initialised (i) before, and (ii) after the  
 198 time of MPES TC genesis (herein after type 1 and type 2 forecast events respectively). A similarity index ( $SI$ ) (Eq.  
 199 14) is used to eliminate type 1 forecast events:

$$200 d_i = \begin{cases} d_{\text{thres}} - d & d < d_{\text{thres}} \\ 0 & d \geq d_{\text{thres}} \end{cases}, \quad (14a)$$

$$201 SI = \frac{\sum_i^{t_{\text{overlap}}} d_i}{d_{\text{thres}} \times t_{\text{overlap}}}, \quad (14b)$$

202 where  $d$  is the great circle distance between position of historical TC and position of TIGGE TC at the overlap  
 203 time step  $i$ ,  $d_{\text{thres}}$  is the maximum tolerance of  $d$ ,  $t_{\text{overlap}}$  is the number of overlap time steps in which both historical  
 204 TC and TIGGE TC existed and it must be larger than 4. Events with  $SI$  larger than  $SI_{\text{thres}}$  are considered as MPES  
 205 TC events. A series of sensitivity study have been done for determining the optimal choice of parameters (not  
 206 shown) and the most optimal setting is  $d_{\text{thres}}=900$  km and  $SI_{\text{thres}} = 0.1$ . Type 2 forecast events are found if the  
 207 separation distance between the position of historical TC and the TIGGE TC at any point of their overlap time is  
 208 less than 400 km. This threshold is determined by the minimum separation between historical TCs and TC in  
 209 JRA-55 event set.

### 210 3.2.4 Detection at Initialisation Filter (DIF)

211 Any events that are detected at the time of model initialisation are removed following Osinski et al. (2016). It is  
 212 because these events are likely to be related to pre-existing disturbances or structures that leads to their  
 213 development. The removal of these events ensures the TPEPS event set is independent of any pre-existing weather  
 214 patterns.

### 215 3.3 Adjustment procedure

216 More than one windstorm event could be found within a close proximity of each other over the WNP. Since the  
 217 clustering algorithm in WiTRACK does not have a maximum size restriction on the cluster, multiple windstorm  
 218 events in close proximity could be identified as one windstorm event by WiTRACK. An additional procedure is  
 219 used to separate these merged windstorm events. This is an iterative procedure which would check whether all  
 220 of the grid boxes at each 6-hourly time step of the windstorm are within 1,000 km radius from the centre of the  
 221 windstorm cluster. If any of the event grid boxes are outside the 1,000 km radius, it will first remove these grid  
 222 boxes and recalculate the centre of event cluster. This procedure is repeated until there is no change in the centre

of cluster. This procedure addresses windstorm event with unrealistically large impact area and event SSI (ESSI).

The event SSI (ESSI) is defined as

$$ESSI = \sum_t^T \sum_k^K \left[ \left( \max \left( 0, \frac{v_{k,t}}{v_{98,k}} - 1 \right) \right)^3 \times A_k \right] \quad (2)$$

where  $v_{k,t}$  is the wind speed at grid box  $k$  and time step  $t$ ,  $v_{98,k}$  is the climatological 98<sup>th</sup> percentile wind speed at grid box  $k$ ,  $A_k$  is the area-dependent weight. Summation is done over all time steps and all grid boxes affected by the windstorm. The threshold radius is chosen to be 1,000 km because typical size of TC wind field is smaller than a circle of 1,000 km radius (Lee et al., 2010; Chan and Chan, 2011).

## 4 Results and discussions

### 4.1 Statistics and Validations

In this section, we present validation of our TPEPS TC event set by comparing the climatological features as provided by a time- and ensemble-aggregated view of the TPEPS TC event set to the historical/reanalysis based event set. A historical TC is said to be detected in a forecast model if there exists a TC counterpart in the forecast model, which is similar to the historical TC as identified by the MTI (c.f. Sect. 3.2.3). The detection rates of historical TCs which are detected in different forecast outputs with at least one MEPS counterpart, i.e. in CMA, ECMWF, JMA, and NCEP, are 91.2%, 94.7%, 89.4%, and 90.7%, respectively, whereas only 54.2% of historical TCs in the period of 2008-2017 are detected in JRA-55 (Table 4). Since WiTRACK is a wind threshold exceedance based detection scheme and the 98<sup>th</sup> percentile wind speed value of JRA-55 within the tropical WNP is similar to these selected TIGGE data (Fig. 1), this implies JRA-55 underestimates the wind speed of wind field of TCs, which is in agreement with Murakami (2014). This also shows these selected TIGGE outputs provide a better representation of the atmosphere. Total 515,712 TC related windstorm events are detected in the selected TIGGE data set. ~38.5% of the all TPEPS events are PEPS TC events (Table 5). Percentage of total TC windstorms as PEPS TCs can be treated as a proxy to quantify the forecast skill of the model. For example, NCEP has 47.1% of TC windstorms as PEPS TCs whereas JMA has 26.5%. This indicates the NCEP model generates more “wrong” forecast than JMA however these “wrong” forecasts are physically possible. Yet, this examining the forecast skill of models is not the focus of this study and the rest of the discussion focuses on the TPEPS TC event set.

Figures 2 and 3 show the spatial pattern and temporal variability of the number of TC which are first detected for each day, respectively, of the TPEPS and JRA-55 event sets. While individual model might have bias in certain spatial and temporal domain, for example the region with the highest track density of JMA is at the eastern WNP in Fig. 31d in comparison to other models, and NCEP failed to capture the peak activity prior 2012 in Fig. 32, the overall patterns of the TPEPS event set match the JRA-55 event set. This is expected because (i) TC formation depends on the environmental conditions and initial disturbance (Gray, 1977; Ritchie and Holland, 1997; Nolan, 2007). During the period of active TC season, environmental conditions over WNP are usually favourable for TC formation but often there is no suitable disturbance in the region. Since EPS simulates the chaotic behaviour of the atmosphere, it would forecast disturbances which would be possible to form but not realised in the real atmosphere. Hence PEPS TCs can be formed in those period of time over WNP. And (ii) the trajectory of TCs depends mainly on the large scale environmental flow of the region (Chan, 2010). This implies

260 PEPS TCs would also follow the typical trajectory of real TCs given that the large scale flow is correctly  
261 represented in the forecast models. Thus, in general the spatial and temporal patterns of the TPEPS event set  
262 match the patterns of JRA-55 event set. There are several possible reasons which lead to the differences in spatial  
263 pattern between TPEPS event set and JRA-55 event set. The eastward bias in the track density appears to be a  
264 common feature in many GCMs (e.g. Camargo et al., 2005; Bell et al., 2013; Roberts et al., 2020), this has also  
265 been observed in seasonal forecast output (Camp et al., 2015). Finite simulation time has also contributed to this  
266 bias as TC that forms in the region east of 150 °E would not have sufficient time to move into the western part of  
267 WNP before the end of simulation time. Differences in number of tracks could also contribute to the differences  
268 in spatial pattern as more diverse tracks would be captured in larger event set.

269 Some TPEPS events appear in locations where no historical TC event is observed (Figs. 2c and 2f).  
270 While there is no historical TC event in some locations, this does not imply TC cannot occur in those regions.  
271 The historical data, which cover 39 years of observations, may not have enough samples to construct a distribution  
272 that can correctly represent the basic population (i.e. all possible TCs in the given climate). For example, the  
273 occurrence of Tropical Storm Vamei that formed close to the equator (~1.4° N) does not satisfy the classical  
274 “necessary but insufficient” conditions of TC formation, which are identified by Gray (1977) based on historical  
275 observations. This shows TC can appear in historically “TC-free” region. Furthermore, from the statistical  
276 perspective, the JRA-55 event set can be viewed as a subset which is randomly selected from the TPEPS event  
277 set. To provide more evidence to support this view, we have conducted bootstrap resampling on the TPEPS event  
278 set to obtain 10,000 sets of subsamples. Each set of subsamples has 668 events to mimic the number of events in  
279 the JRA-55 event set. Uncentred pattern correlation between the track density of the JRA-55 event set and the  
280 track density of each set of subsamples are calculated. In order to focus on the relevant entries, if the values of  
281 track density of a grid box for a resampling set and the JRA-55 event set are both less than 1, such grid box is  
282 neglected in the pattern correlation calculation. The mean, standard deviation, minimum and maximum of the  
283 uncentred pattern correlation of the 10,000 set of subsamples are 0.9380, 0.0107, 0.8961, and 0.9697, respectively.  
284 This suggests the spatial pattern of the JRA-55 event set is highly similar to some small random subsets of the  
285 TPEPS event set. Thus, the JRA-55 event set can be seen as a subset which is randomly selected from the  
286 TPEPS event set. On the other hand, it is not possible to deduce the basic population (e.g. the TPEPS event  
287 set) from a small sample set (e.g. the JRA-55 event set). Although the spatial distribution of the small set sample  
288 is similar to the subsamples of the basic population and thus usable as one possible realisation of the basic  
289 population, the small sample set does not contain all of the information of the underlying population. Furthermore,  
290 the statistical estimate of extremes would also be different for the small sample set and the basic population.

291 The spatial discrepancy near the dateline between the JRA-55 event set and the TPEPS event set (Figs. 2e and 2f)  
292 can be explained by considering the amount of data used in the construction of event sets. The JRA-55 event set  
293 is constructed based on 39 year of reanalysis data whereas the TPEPS event set is constructed using more than  
294 40,000 years of TC model data from operational forecast models. Since both event sets are constructed from  
295 physical models (i.e. GCMs), the JRA-55 event set can be considered as a subset of the TIGGE event set.  
296 Furthermore, in the region 0–20 °N and 160–180 °E, the 98<sup>th</sup> percentile values of JRA-55 is higher than all TIGGE  
297 models considered in this study (Fig. 1). Consequently, systems with the same strength would be identified in  
298 that region in the TPEPS event set but not in the JRA-55 event set.

299 Some of the examples of TPEPS TC tracks and impact footprints are shown in Fig. 4. The trajectory of  
300 these TPEPS TC tracks is indistinguishable to historical TC trajectories in WNP. This shows these TPEPS TC  
301 events are realistic and physically possible events. Figure 5 shows the climatological daily number distributions  
302 of TC first detections for TPEPS TC event set and JRA-55 event set. Although the peak activities period of JMA  
303 is slightly lagged behind and the over- and under-estimation of the peak of activity for CMA and NCEP are  
304 observed, respectively, the seasonal cycle of TPEPS TC event set is well captured and this matches to the seasonal  
305 cycle of the JRA-55 event set. This shows our new approach is capable to produce spatially and temporally  
306 realistic events.

307 In general, the temporal evolutions of the number of first storm detections of TPEPS event set during the  
308 integration time has an increasing trend in the short lead time followed by a roughly constant behaviour (Fig. 6).  
309 In short lead time (i.e. close to initialisation of forecast), the true state of the atmosphere is well simulated by  
310 forecast models, thus EPSs are likely to produce storms that actually occurred (i.e. MEPS storms) and less likely  
311 to produce PEPS storms (Osinski et al., 2016). As lead time increases, more PEPS storms are produced due to  
312 increasing uncertainty of the state and the chaotic behaviour of the atmosphere in EPSs. When EPS has no  
313 memory of the initialisation state of the atmosphere, the probability distribution of formation of PEPS TCs  
314 becomes a uniform distribution.

315 The overall impact of any storm is related to the many factors for example lifetime of the storm, the size  
316 of the storm, and the intensity (or strength) of the storm (e.g. Vickery et al., 2000; Mori and Takemi, 2016; Kim  
317 and Lee, 2019). Here we investigate whether there are systematic biases in the TPEPS TC event set which would  
318 affect these quantities. The lifetime distribution of TPEPS TCs matches to the JRA-55 event set but proportionally  
319 overestimates for short-lived TCs and underestimates for long-lived TCs (Fig. 7a). These differences are the  
320 consequence of the finite simulation time in forecast models. If the same restriction (i.e. finite simulation time  
321 window) is applied to the JRA-55 TC event set (grey shaded areas in Fig. 7), the lifetime distribution of TPEPS  
322 TCs would be in good agreement to the JRA-55 TCs. Similar conclusion can be reached in the comparison of the  
323 distribution of time required to reach lifetime maximum intensity (LMI) (Fig. 7b). However, finite simulation  
324 time of EPSs cannot explain the difference in the distribution of impact area, which is the total area that has  
325 experienced TC-associated extreme wind (i.e. larger than local climatological 98<sup>th</sup> percentile wind speed), between  
326 TPEPS and JRA-55 event sets despite they have the same type of distribution (Fig. 7c). The difference in the  
327 distributions of impact area maybe due to the fact that wind speed of the TC wind fields is underestimated in JRA-  
328 55 as discussed above. Consequently, many weaker TCs, which would have small impact areas, are not detected  
329 and thus they are not necessarily included in the JRA-55 TC event set.

#### 330 4.2 Robust TC hazard risk assessment

331 To demonstrate the benefit of our approach, TC records in IBTrACS, JRA-55 TC event set, and TPEPS TC event  
332 set are stratified into intensity classes according to their lifetime maximum intensity (c.f. Table 6). Since  
333 WiTRACK is an impact-oriented, wind speed percentile based tracking scheme which tracks TCs with potential  
334 impact (Befort et al., 2020), many of the low impact TCs (i.e. TCs in the Tropical Depression and Tropical  
335 Storm (TD&TS) category) are not detected and thus not included in the TPEPS TC event set. Focusing onto the  
336 categories of high impact TC, i.e. Typhoon (TY), Very Strong Typhoon (VST), and Violent Typhoon (VTY), the

337 TPEPS event set contains 302.14, 102.54, and 77.02 times more TY, VST, and VTY than the IBTrACS records,  
338 respectively. This means our new approach can capture much more extremely high impact events such that a  
339 more robust analysis of extreme TC events can be done.

340 The key advantage of this new approach is that it constructs a physically consistent and high information  
341 content TC event set with good and realistic representation of the current climate state using a computationally  
342 inexpensive algorithm. Since more physically consistent and physically possible TCs are included, more extreme  
343 events can be captured in the TPEPS event set. Consequently, a robust TC **hazard risk** assessment can be obtained.  
344 Some of the examples are presented in this subsection.

345 Figure 8 shows the location of first detection of TCs with LMI at least typhoon strength, which made  
346 landfall within the given domain (105-180° E, 0-30° N) for TPEPS and JRA-55 TC event set. The spatial pattern  
347 of the TPEPS TC event set (Fig. 8f) matches the spatial pattern of the JRA-55 TC event set. The data in the JRA-  
348 55 TC event set are sparse and it does not provide sufficient information about whether TCs, which made landfall  
349 in this region, are typically first identified in the WNP or in the South China Sea (SCS). **The TPEPS TC** event  
350 set, on the other hand, provides a clearer picture and suggests events, which made landfall in this domain, are  
351 typically first identified in the SCS and western WNP. This is consistent with the known climatology. As TCs  
352 within the SCS and western WNP usually follow the western and northwestern trajectory and subsequently made  
353 landfall over the Vietnam, south and southeast mainland China, Taiwan, and the Philippines.

354 Figure 9 shows the number of TC landfall events, which made landfall with at least typhoon strength,  
355 with the focus of southern and southeast mainland China, and Taiwan. Much more landfall events have been  
356 captured by TPEPS TC event set (11449) than the JRA-55 TC event set (100). The spatial distribution of TPEPS  
357 TCs is in good agreement with the JRA-55 TCs **with uncentred pattern correlation of 0.8345**. TCs, which made  
358 landfall with at least typhoon strength, are more likely to made landfall along the coast of the southern Fujian  
359 Province and the eastern Guangdong Province than any other coastal area of South and Southeast mainland China.  
360 Furthermore, higher TC landfall frequency is observed on the side of islands (i.e. Hainan Island and Taiwan)  
361 which faces the open ocean than the other side of islands. This is consistent with observations. The TPEPS TC  
362 event set also provides information about the frequency of TC landfall at locations where no landfall events had  
363 observed in the JRA-55 TC event set, e.g. locations along the coastline of Guangdong Province. **Furthermore, the**  
364 **distribution of landfall intensity for TCs, which made landfall with at least typhoon strength, for the TPEPS TC**  
365 **event set is very similar to the JRA-55 TC event set (the null hypothesis, i.e. the distributions are the same, is not**  
366 **rejected at the 0.05 significance level of the two-sample Kolmogorov-Smirnov test).**——

### 367 4.3 Application

368 The TPEPS TC event set is constructed based on physical models, i.e. GCMs, which provide a good representation  
369 of the atmosphere of the real world. The wind field associates to a TPEPS TC event is realistic and local effects,  
370 such as local topography, have been taken into account. This implies the wind information of the TPEPS TC  
371 event set can be used for estimates return periods of local extreme wind events associated with typhoon with high  
372 confidence. **F**igure 10 shows the number of TC-related 6-hourly extreme wind (i.e. wind speed higher than the  
373 local 98<sup>th</sup> percentile climatological wind speed) data entries in each of the grid box within Guangdong Province  
374 in the Southern China. The JRA-55 TC event set can only construct a TC-related 6-hourly extreme distribution

375 with ~25 (inland) and ~325 (coastal) data entries whereas such distribution can be constructed with at least 500  
376 to over 28,000 data entries using the TPEPS TC event set. This implies the estimated return period using the  
377 TPEPS TC event set would be more reliable than using the JRA-55 TC event set and similarly the observation  
378 data alone. This is of importance from the DRR perspective as wind speed values are used in practice to decide  
379 on payments out of parametric insurance products (Swiss Re, 2016). Consequently, reliable wind-based trigger  
380 points of typhoon parametric insurance can be determined. This will further improve the suitability and flexibility  
381 of parametric insurance for DRR applications. Ultimately, this will improve the speed of post-disaster recovery.  
382 A demonstration for such calculation application is given below. This is demonstrated as follows.

383 Four surface observation stations are chosen for this demonstration, they are Baiyun International Airport  
384 (BAIYUN INTL; 23.392° N, 113.299° E; from 1945-2019), Baoan International Airport (BAOAN INTL; 22.639°  
385 N, 113.811° E; from 1957-2019), Shanwei (22.783° N, 115.367° E; from 1956-2019), and Shangchuan Dao  
386 (21.733° N, 112.767° E; from 1959-2019). For each selected surface station, the grid box of each EPS that  
387 corresponds to the surface station is identified (Fig.11). Resolution of models is known to be a factor to limit the  
388 wind speed of TCs (Bengtsson et al., 2007). This means for the same TC, the associated wind speed would be  
389 lower in low resolution model and higher for high resolution model. In order to utilise the extreme wind  
390 information from EPSs with different resolution, the cube of 98<sup>th</sup> percentile relative exceedance of wind speed  
391 (EXCE) is used. Since EXCE is a ratio, it is a resolution independent quantity and the tail behaviours of the  
392 EXCE distribution for these models are similar, which is in agreement with Osinski et al. (2016). Information  
393 from different models can be combined using EXCE. EXCE entries, which correspond to TC in the TPEPS TC  
394 event set, are extracted for those grid boxes. This forms a set of “observations” of the impacts of high impact TCs  
395 at those grid boxes in the model space. We assume all of the EXCE entries are independent and identically  
396 distributed (iid) random variables. This is a reasonable assumption, due to the fast moving nature of TCs, diverse  
397 possible direction of the movement of wind field, and rapid decay of wind field over land for a 6-hour interval,  
398 local observations often have only one extreme wind observations ~~for~~ a TC event. In order to translate this  
399 information to the physical world, quantile mapping is used for mapping EXCE to the observed surface wind  
400 speed which exceeded local climatological 98<sup>th</sup> percentile. Historical in situ surface wind data are obtained from  
401 the Integrated Surface Database (ISD) (Smith et al., 2011). Quantile mapping is done using the R package *qmap*  
402 (Gudmundsson et al., 2012; Gudmundsson, 2016). Due to different geographic configuration and climatology of  
403 each in situ observation station, different quantile mapping strategies have been employed. The optimal strategy  
404 is chosen based on minimisation of the root-mean-square-error (RMSE) of the quantile mapping output (see  
405 Gudmundsson (2016) for more details). Using above information, the return period-return level plot (using  
406 threshold exceedance approach) is constructed using the R package *extRemes* (Gilleland and Katz, 2016). For  
407 detail discussion of calculation of return period and return level, readers are referred to Elsner et al. (2006), Jagger  
408 and Elsner (2006), and Gilleland and Katz (2016). Figure 12 shows the return period-return level plot of four  
409 selected stations which are derived using our proposed approach with the TPEPS TC event set and using in situ  
410 observational data. The width of the 95% confidence interval which is calculated using our proposed approach is  
411 much sharper than the 95% confidence interval which is calculated using in situ observational data. In other  
412 words, the uncertainty can be reduced by using the TPEPS TC event set because more observations are used in  
413 the calculation.

414 The above application of the TPEPS TC event set can provide crucial information for the DRR  
415 community. As discussed in the introduction, typhoon parametric insurance can be an effective financial  
416 instrument for typhoon risk transfer. However, an effective typhoon parametric insurance requires a robust trigger  
417 point, which is determined by the meteorological information, e.g. wind speed. If the trigger point is too high,  
418 disbursements would not be made even if a catastrophic meteorological disaster has occurred, i.e. under-  
419 compensation; If the trigger point is too low, disbursements would be made even if no catastrophic event has  
420 occurred. Using the TPEPS TC event set, the estimated return period has smaller uncertainty than the estimation  
421 made by in situ observational data, such that an optimal trigger point for typhoon parametric insurance can be  
422 determined.

## 423 5 Summary and Conclusions

424 In this study, a new and efficient method, which addresses the critical issue in typhoon risk assessments – a robust  
425 methodology to determine the real frequency of TC occurrence with high socioeconomic impact potential by  
426 constructing a physically consistent TC event set, is presented to produce a physically consistent TC event set  
427 with high information content in the WNP has been presented. This is achieved by applying an objective impact-  
428 oriented windstorm identification algorithm – WiTRACK, on 6-hourly 10-m horizontal wind field of selected  
429 ensemble data set from a multi-centre grand ensemble data archive – TIGGE. While WiTRACK identifies major  
430 events based on one meteorological variable only, it is capable of identifying events of general loss relevance as  
431 demonstrated by Bafort et al. (2020). This implies the event set generated by our approach is in principle suitable  
432 for general TC risk assessments, as well as for an assessment of the hazards frequency-intensity distribution  
433 specifically. Bafort et al. (2020) Several sensitivity tests with different parameter settings are done using JRA-55  
434 data to obtain the optimal setup for WiTRACK. Since WiTRACK can identify all types of windstorm events,  
435 ~~4~~four post-processing procedures are used to identify PEPS TCs, these procedures include a geographic filter and  
436 logistics regression classifier. The TPEPS event set has the climatological spatial and temporal pattern of TCs  
437 which match to the historical climatological pattern of TC in WNP. More than 302, 102, and 77 times of TY,  
438 VSTY, and VTY, respectively, are found in the TPEPS TC event set in comparison to the IBTrACS record. A  
439 robust representation of extreme TC events in WNP can be obtained using the TPEPS TC event set because of the  
440 high number of physically consistent extreme events. Consequently, a robust hazard ~~risk~~-assessment of land-  
441 affecting ~~typhoons~~-TCs in the WNP can be produced using the event set constructed by this new method.  
442 Furthermore, the return-period of typhoon-related extreme wind events e.g. Typhoon Haiyan (2013) and Typhoon  
443 Mangkhut (2018), can be determined with sharper confidence intervals in a similar manner as Walz and  
444 Leckebusch (2019). As a result, policymakers and related stakeholders can improve the current typhoon related  
445 disaster reduction and mitigation strategy. ~~Furthermore~~Furthermore, a robust trigger point for parametric typhoon  
446 hazard insurance can be determined using our proposed approach by reducing the uncertainty of estimated return  
447 period of a meteorological extreme event. This will improve the suitability and flexibility of parametric insurance  
448 for DRR applications. Consequently, this will improve the speed of post-disaster recovery.

449 The TC event set constructed using the method described in this ~~study~~paper has several unique properties  
450 in comparison to the TC event set constructed by other methods (Vickery et al., 2000; Emanuel et al., 2006; Rumpf  
451 et al., 2009; Kim and Lee, 2019):

452 (i) Many methods in the literature (e.g. Emanuel et al., 2006; Rumpf et al., 2009) use historical best track data  
453 to construct a spatial probability function that determine the genesis location of synthetic TCs and a parametric  
454 track model, that matches to the historical observations, to determine the movement of synthetic TCs.  
455 Consequently, these synthetic tracks are highly likely to be identified in the region where TCs were identified  
456 from the historical observations and highly ~~unlikely-rare~~ in the region where TCs were never identified but  
457 physically possible. In contrast, TPEPS TCs are detected at any physically possible locations over the WNP. This  
458 means, besides the events, which are similar to the historical observations, the TPEPS TC event set also includes  
459 events that occur in the region where no historical event was observed. There are two underlying reasons: (1) The  
460 physical reason—TC has low probability of occurrence in those regions due to typical unfavourable environment.  
461 For example, following the classical “necessary but insufficient” conditions of TC formation which are identified  
462 by ; (2) The statistical reason—the observation period is too short and it does not provide enough samples for the  
463 underlying population. Consequently, the TPEPS TC event set provides an important and unique advantage for  
464 typhoon hazard risk assessment. In comparison to other methods to generate large TC event sets, our specific  
465 approach is limited mainly by the source of data used. The current TC event set constructed using medium range  
466 forecasts archived in TIGGE, is strictly spoken representative only for the current climate state. Any longer-term  
467 climate variability (e.g. multi-decadal fluctuations like the Pacific Decadal Oscillation (PDO)) and their impacts  
468 on any TC frequency-intensity distribution are not accounted for in this setting. Nevertheless, the presented  
469 approach would be equally applicable to data sets representing that kind of variability on longer time scales (e.g.  
470 decadal predictions or transient climate model simulations).

471

472

473 ~~These events are typically associated with low probability of occurrence, yet, they are still physically possible.~~

474 ~~The TPEPS event set includes events which are unlikely but physically possible. This~~  
475 ~~provides an important and unique advantage for typhoon risk assessment.~~

476 (ii) In the literature, the structure of wind field of synthetic TCs follows a predefined, analytical model, e.g.  
477 parametric vortex structure developed by Holland (1980) or modified Rankine vortex. For the TPEPS TC event  
478 set, complex physical processes in GCMs determine the structure of wind field of TCs, therefore the structure of  
479 wind field of TCs is realistic. This is an advantage for robust wind hazard risk assessment of land-affecting TCs  
480 because the resultant wind field includes the complex atmosphere-land interaction which depends on the local  
481 topography. Consequently, the TPEPS TC event set can be used as addition observations for the estimation of  
482 return period of TC-related extreme wind as demonstrated above.

483 (iii) Many of the TC risk assessments are done based on wind risk, and/or wind-induced coastal risk but not  
484 TC-related precipitation risk (Vickery et al., 2000; Emanuel et al., 2006; Rumpf et al., 2009; Mendelsohn et al.,  
485 2012; Mori and Takemi, 2016; Marsooli et al., 2019; Kim and Lee, 2019). A reason is that historical damages  
486 due to TC-related wind are much better documented than TC-related precipitation damages (Emanuel et al., 2006).  
487 However, damages due to TC-related precipitation, e.g. flooding, should not be ignored. Based on the pay-out of  
488 the National Flood Insurance Program of the United States for the flood event of Hurricane Ike (2008), Smith and  
489 Katz (2013) estimated the insured flood damage as 5.3764 billion USD. Furthermore, some of the high impact



490 TCs in WNP have typical typhoon intensity but the amount of rainfall is extremely high, e.g. Typhoon Morakot  
491 (2009) (Wu, 2012). Since precipitation is one of the output variables of these medium range ensemble forecasts,  
492 precipitation-related impact can be examine by integrating the realistic precipitation information from forecast  
493 outputs into the TPEPS TC event set. Furthermore a spatial distribution of TC related hazard, e.g. extreme wind  
494 and extreme precipitation, of the TPEPS TC event set can be constructed using the notion of TC hazard footprint  
495 (Chen et al., 2018). Consequently, a more thorough typhoon risk assessment can be achieved. This is currently  
496 under our investigation.

497 In conclusion, the event set that we have constructed contains all necessary information for applications  
498 in the DRR context. This event set can improve the hazard component in an overall assessment of integrated TC  
499 risks (e.g. Sajjad and Chan, 2019) by providing a robust probability of occurrence of extreme TC event.  
500 Furthermore, using this event set, a robust trigger points of parametric insurance for the local hazard can be  
501 determined. Once such trigger points for the local hazard are available (including their uncertainty), the targeted  
502 application of parametric insurance products in disaster relief application is possible. Especially, when it comes  
503 to the evaluation of the basis risk. This study is merely the first step toward a statistically robust, full physical  
504 model based TC hazard assessment. The impact of TC-related extreme precipitation and storm surges can be  
505 integrated following the approach developed by Befort et al. (2015).

506  
507

508

509 *Data availability.* JRA-55 (Kobayashi et al., 2015) and ERA-I (Dee et al., 2011) are freely available for academic  
510 use at the UCAR Research Data Archive: <https://rda.ucar.edu/datasets>. The TIGGE dataset (Bougeault et al.,  
511 2010; Swinbank et al., 2015) used in this study can be accessed through ECMWF server:  
512 <https://apps.ecmwf.int/datasets/data/tigge/levtype=sfc/type=pf/>. IBTrACS (Knapp et al., 2010) and ISD (Smith  
513 et al., 2011) are available at the United States National Centers for Environmental Information, National oceanic  
514 and Atmospheric Administration: <https://www.ncdc.noaa.gov/ibtracs/index.php>, and  
515 <https://www.ncdc.noaa.gov/isd>, respectively. JTWC best track data used in this study is obtained from the United  
516 States Navy Website: <https://www.metoc.navy.mil/jtwc/jtwc.html?best-tracks>.

517

518 *Author contribution.* KSN and GCL originated the idea, developed the methodology, performed data analysis, and  
519 wrote the paper.

520

521 *Competing interests.* The authors declare that they have no conflict of interest.

522

523 *Acknowledgments.* The authors thank three reviewers for their helpful and constructive comments. The authors  
524 thank Drs. D. Befort and M. Angus for valuable discussion. This work was supported by the Building Resilience

525 to Natural Disasters using Financial Instruments grant INPAIS (Integrated Threshold Development for Parametric  
526 Insurance Solutions for Guangdong Province China, Grant Ref: NE/R014264/1, through Natural Environment  
527 Research Council (NERC). The computations described in this paper were performed using the BlueBEAR HPC  
528 service at the University of Birmingham.

## 529 **References**

- 530 Bakkensen, L. A., Shi, X., and Zurita, B. D.: The Impact of Disaster Data on Estimating Damage Determinants  
531 and Climate Costs, *Economics of Disasters and Climate Change*, 2, 49-71, 10.1007/s41885-017-0018-x,  
532 2018.
- 533 Befort, D. J., Fischer, M., Leckebusch, G. C., Ulbrich, U., Ganske, A., Rosenhagen, G., and Heinrich, H.:  
534 Identification of storm surge events over the German Bight from atmospheric reanalysis and climate  
535 model data, *Natural Hazards and Earth System Sciences*, 15, 1437, 2015.
- 536 Befort, D. J., Wild, S., Kruschke, T., Ulbrich, U., and Leckebusch, G. C.: Different long-term trends of extra-  
537 tropical cyclones and windstorms in ERA-20C and NOAA-20CR reanalyses, *Atmos Sci Lett*, 17, 586-  
538 595, 10.1002/asl.694, 2016.
- 539 Befort, D. J., Wild, S., Knight, J. R., Lockwood, J. F., Thornton, H. E., Hermanson, L., Bett, P. E., Weisheimer,  
540 A., and Leckebusch, G. C.: Seasonal forecast skill for extratropical cyclones and windstorms, *Q J Roy  
541 Meteor Soc*, 145, 92-104, 10.1002/qj.3406, 2019.
- 542 Befort, D. J., Kruschke, T., and Leckebusch, G. C.: Objective identification of potentially damaging tropical  
543 cyclones over the Western North Pacific, *Environmental Research Communications*, 2, 031005,  
544 10.1088/2515-7620/ab7b35, 2020.
- 545 Belanger, J. I., Webster, P. J., Curry, J. A., and Jelinek, M. T.: Extended Prediction of North Indian Ocean Tropical  
546 Cyclones, *Weather and Forecasting*, 27, 757-769, 10.1175/WAF-D-11-00083.1, 2012.
- 547 Bell, R., Strachan, J., Vidale, P. L., Hodges, K., and Roberts, M.: Response of Tropical Cyclones to Idealized  
548 Climate Change Experiments in a Global High-Resolution Coupled General Circulation Model, *J  
549 Climate*, 26, 7966-7980, 10.1175/JCLI-D-12-00749.1, 2013.
- 550 Bengtsson, L., Hodges, K. I., and Esch, M.: Tropical cyclones in a T159 resolution global climate model:  
551 Comparison with observations and re-analyses, *Tellus A*, 59, 396-416, 2007.
- 552 Bougeault, P., Toth, Z., Bishop, C., Brown, B., Burridge, D., Chen, D. H., Ebert, B., Fuentes, M., Hamill, T. M.,  
553 Mylne, K., Nicolau, J., Paccagnella, T., Park, Y.-Y., Parsons, D., Raoult, B., Schuster, D., Dias, P. S.,  
554 Swinbank, R., Takeuchi, Y., Tennant, W., Wilson, L., and Worley, S.: The THORPEX Interactive Grand  
555 Global Ensemble, *B Am Meteorol Soc*, 91, 1059-1072, 10.1175/2010BAMS2853.1, 2010.
- 556 Buckingham, C., Marchok, T., Ginis, I., Rothstein, L., and Rowe, D.: Short- and Medium-Range Prediction of  
557 Tropical and Transitioning Cyclone Tracks within the NCEP Global Ensemble Forecasting System,  
558 *Weather and Forecasting*, 25, 1736-1754, 10.1175/2010WAF2222398.1, 2010.
- 559 Camargo, S. J., Barnston, A. G., and Zebiak, S. E.: A statistical assessment of tropical cyclone activity in  
560 atmospheric general circulation models, *Tellus A*, 57, 589-604, 10.1111/j.1600-0870.2005.00117.x,  
561 2005.
- 562 Camp, J., Roberts, M., MacLachlan, C., Wallace, E., Hermanson, L., Brookshaw, A., Arribas, A., and Scaife, A.  
563 A.: Seasonal forecasting of tropical storms using the Met Office GloSea5 seasonal forecast system, *Q J  
564 Roy Meteor Soc*, 141, 2206-2219, 10.1002/qj.2516, 2015.
- 565 Cavallo, E., and Noy, I.: Natural Disasters and the Economy — A Survey, *International Review of Environmental  
566 and Resource Economics*, 5, 63-102, 10.1561/101.00000039, 2011.
- 567 Chan, J. C. L.: Movement of Tropical Cyclones, in: *Global Perspectives on Tropical Cyclones*, World Scientific  
568 Series on Asia-Pacific Weather and Climate, Volume 4, World Scientific, 133-148, 2010.
- 569 Chan, K. T. F., and Chan, J. C. L.: Size and Strength of Tropical Cyclones as Inferred from QuikSCAT Data, *Mon  
570 Weather Rev*, 140, 811-824, 10.1175/MWR-D-10-05062.1, 2011.
- 571 Chen, W., Lu, Y., Sun, S., Duan, Y., and Leckebusch, G. C.: Hazard Footprint-Based Normalization of Economic  
572 Losses from Tropical Cyclones in China During 1983–2015, *International Journal of Disaster Risk  
573 Science*, 9, 195-206, 10.1007/s13753-018-0172-y, 2018.
- 574 CMA: Member report, ESCAP/WMO Typhoon Committee 13th Integrated Workshop, 36, 2018.
- 575 Dee, D. P., Uppala, S. M., Simmons, A. J., Berrisford, P., Poli, P., Kobayashi, S., Andrae, U., Balmaseda, M. A.,  
576 Balsamo, G., Bauer, P., Bechtold, P., Beljaars, A. C. M., van de Berg, L., Bidlot, J., Bormann, N., Delsol,  
577 C., Dragani, R., Fuentes, M., Geer, A. J., Haimberger, L., Healy, S. B., Hersbach, H., Hólm, E. V.,  
578 Isaksen, L., Kållberg, P., Köhler, M., Matricardi, M., McNally, A. P., Monge-Sanz, B. M., Morcrette, J.  
579 J., Park, B. K., Peubey, C., de Rosnay, P., Tavalato, C., Thépaut, J. N., and Vitart, F.: The ERA-Interim

580 reanalysis: configuration and performance of the data assimilation system, *Q J Roy Meteor Soc*, 137,  
581 553-597, 10.1002/qj.828, 2011.

582 Desai, B., Maskrey, A., Peduzzi, P., De Bono, A., and Herold, C.: Making Development Sustainable: The Future  
583 of Disaster Risk Management, Global Assessment Report on Disaster Risk Reduction, United Nations  
584 Office for Disaster Risk Reduction (UNISDR), Genève, Suisse, Geneva: UNISDR, 2015.

585 Elsner, J. B., Jagger, T. H., and Tsonis, A. A.: Estimated return periods for Hurricane Katrina, *Geophys Res Lett*,  
586 33, 10.1029/2005GL025452, 2006.

587 Emanuel, K.: Climate and tropical cyclone activity: A new model downscaling approach, *J Climate*, 19, 4797-  
588 4802, Doi 10.1175/Jcli3908.1, 2006.

589 Emanuel, K., Ravela, S., Vivant, E., and Risi, C.: A statistical deterministic approach to hurricane risk assessment,  
590 *B Am Meteorol Soc*, 87, 299-314, 10.1175/Bams-87-3-299, 2006.

591 Gilleland, E., and Katz, R. W.: extRemes 2.0: An Extreme Value Analysis Package in R, *Journal of Statistical*  
592 *Software*; Vol 1, Issue 8 (2016), 10.18637/jss.v072.i08, 2016.

593 Glauber, J. W.: Crop Insurance Reconsidered, *American Journal of Agricultural Economics*, 86, 1179-1195,  
594 10.1111/j.0002-9092.2004.00663.x, 2004.

595 Gray, W. M.: Tropical Cyclone Genesis in the Western North Pacific, *J Meteorol Soc Jpn*, 55, 465-482, 1977.

596 Gudmundsson, L., Bremnes, J. B., Haugen, J. E., and Engen-Skaugen, T.: Technical Note: Downscaling RCM  
597 precipitation to the station scale using statistical transformations &ndash; a comparison of methods,  
598 *Hydrol. Earth Syst. Sci.*, 16, 3383-3390, 10.5194/hess-16-3383-2012, 2012.

599 Gudmundsson, L.: qmap: Statistical transformations for post-processing climate model output. R package version  
600 1.0-4. 2016.

601 Halperin, D. J., Fuelberg, H. E., Hart, R. E., Cossuth, J. H., Sura, P., and Pasch, R. J.: An Evaluation of Tropical  
602 Cyclone Genesis Forecasts from Global Numerical Models, *Weather and Forecasting*, 28, 1423-1445,  
603 10.1175/WAF-D-13-00008.1, 2013.

604 Hamill, T. M., Whitaker, J. S., Fiorino, M., and Benjamin, S. G.: Global Ensemble Predictions of 2009's Tropical  
605 Cyclones Initialized with an Ensemble Kalman Filter, *Mon Weather Rev*, 139, 668-688,  
606 10.1175/2010MWR3456.1, 2010.

607 Hart, R. E.: A cyclone phase space derived from thermal wind and thermal asymmetry, *Mon Weather Rev*, 131,  
608 585-616, Doi 10.1175/1520-0493(2003)131<0585:Acpsdf>2.0.Co;2, 2003.

609 Hastie, T., Tibshirani, R., and Friedman, J.: *The Elements of Statistical Learning*, Springer Series in Statistics,  
610 Springer-Verlag New York, 745 pp., 2009.

611 Holland, G. J.: An Analytic Model of the Wind and Pressure Profiles in Hurricanes, *Mon Weather Rev*, 108, 1212-  
612 1218, 10.1175/1520-0493(1980)108<1212:AAMOTW>2.0.CO;2, 1980.

613 IPCC: *Managing the risks of extreme events and disasters to advance climate change adaptation*, Cambridge, A  
614 special report of Working Groups I and II of the Intergovernmental Panel on Climate Change, 2012.

615 Jagger, T. H., and Elsner, J. B.: Climatology Models for Extreme Hurricane Winds near the United States, *J*  
616 *Climate*, 19, 3220-3236, 10.1175/JCLI3913.1, 2006.

617 Jing, R., and Lin, N.: An Environment-Dependent Probabilistic Tropical Cyclone Model, *J Adv Model Earth Sy*,  
618 12, e2019MS001975, 10.1029/2019MS001975, 2020.

619 Kim, G. Y., and Lee, S.: Prediction of extreme wind by stochastic typhoon model considering climate change,  
620 *Journal of Wind Engineering and Industrial Aerodynamics*, 192, 17-30, 10.1016/j.jweia.2019.05.003,  
621 2019.

622 Knapp, K. R., Kruk, M. C., Levinson, D. H., Diamond, H. J., and Neumann, C. J.: The International Best Track  
623 Archive for Climate Stewardship (IBTrACS) Unifying Tropical Cyclone Data, *B Am Meteorol Soc*, 91,  
624 363-376, Doi 10.1175/2009bams2755.1, 2010.

625 Kobayashi, S., Ota, Y., Harada, Y., Ebata, A., Moriya, M., Onoda, H., Onogi, K., Kamahori, H., Kobayashi, C.,  
626 Endo, H., Miyaoka, K., and Takahashi, K.: The JRA-55 Reanalysis: General Specifications and Basic  
627 Characteristics, *Journal of the Meteorological Society of Japan. Ser. II*, 93, 5-48, 10.2151/jmsj.2015-001,  
628 2015.

629 Kruschke, T.: Winter wind storms: Identification, verification of decadal predictions, and regionalization, *Doktors*  
630 *der Naturwissenschaften, Institut für Meteorologie, Freie Universität Berlin*, 181 pp., 2015.

631 Kuhn, M., Wing, J., Weston, S., Williams, A., Keefer, C., Engelhardt, A., Cooper, T., Mayer, Z., Kenkel, B.,  
632 Benesty, M., Lescarbeau, R., Ziem, A., Scrucca, L., Tang, Y., Candan, C., and Hunt, T.: *Classification*  
633 *and Regression Training*. 2018.

634 Leckebusch, G. C., Renggli, D., and Ulbrich, U.: Development and Application of an Objective Storm Severity  
635 Measure for the Northeast Atlantic Region, *Meteorologische Zeitschrift*, 17, 575-587, 10.1127/0941-  
636 2948/2008/0323, 2008.

637 Lee, C.-S., Cheung, K. K. W., Fang, W.-T., and Elsberry, R. L.: Initial Maintenance of Tropical Cyclone Size in  
638 the Western North Pacific, *Mon Weather Rev*, 138, 3207-3223, 10.1175/2010MWR3023.1, 2010.

639 Lee, C.-Y., Tippett, M. K., Sobel, A. H., and Camargo, S. J.: An Environmentally Forced Tropical Cyclone Hazard  
640 Model, *J Adv Model Earth Sy*, 10, 223-241, 10.1002/2017MS001186, 2018.

641 Lemcke, G.: A resilient world: NatCat parametric insurance solutions for China's Provincial Government, Sigma  
642 event 2017: Catastrophes-Protecting the uninsured. Solutions for a resilient world, Zurich, Switzerland,  
643 6-7 April, 2017.

644 Leonardo, N. M., and Colle, B. A.: Verification of Multimodel Ensemble Forecasts of North Atlantic Tropical  
645 Cyclones, *Weather and Forecasting*, 32, 2083-2101, 10.1175/WAF-D-17-0058.1, 2017.

646 Luitel, B., Villarini, G., and Vecchi, G. A.: Verification of the skill of numerical weather prediction models in  
647 forecasting rainfall from U.S. landfalling tropical cyclones, *Journal of Hydrology*, 556, 1026-1037,  
648 10.1016/j.jhydrol.2016.09.019, 2018.

649 Magnusson, L., Bidlot, J.-R., Lang, S. T. K., Thorpe, A., Wedi, N., and Yamaguchi, M.: Evaluation of Medium-  
650 Range Forecasts for Hurricane Sandy, *Mon Weather Rev*, 142, 1962-1981, 10.1175/MWR-D-13-  
651 00228.1, 2014.

652 Majumdar, S. J., and Torn, R. D.: Probabilistic Verification of Global and Mesoscale Ensemble Forecasts of  
653 Tropical Cyclogenesis, *Weather and Forecasting*, 29, 1181-1198, 10.1175/WAF-D-14-00028.1, 2014.

654 Marsooli, R., Lin, N., Emanuel, K., and Feng, K.: Climate change exacerbates hurricane flood hazards along US  
655 Atlantic and Gulf Coasts in spatially varying patterns, *Nature Communications*, 10, 3785,  
656 10.1038/s41467-019-11755-z, 2019.

657 Mendelsohn, R., Emanuel, K., Chonabayashi, S., and Bakkensen, L.: The impact of climate change on global  
658 tropical cyclone damage, *Nature Climate Change*, 2, 205-209, 10.1038/nclimate1357, 2012.

659 Mori, N., and Takemi, T.: Impact assessment of coastal hazards due to future changes of tropical cyclones in the  
660 North Pacific Ocean, *Weather and Climate Extremes*, 11, 53-69, 10.1016/j.wace.2015.09.002, 2016.

661 Murakami, H.: Tropical cyclones in reanalysis data sets, *Geophys Res Lett*, 41, 2133-2141,  
662 10.1002/2014GL059519, 2014.

663 Nissen, K. M., Ulbrich, U., Leckebusch, G. C., and Kuhnel, I.: Decadal windstorm activity in the North Atlantic-  
664 European sector and its relationship to the meridional overturning circulation in an ensemble of  
665 simulations with a coupled climate model, *Climate Dynamics*, 43, 1545-1555, 10.1007/s00382-013-  
666 1975-6, 2014.

667 Nolan, D. S.: What is the trigger for tropical cyclogenesis?, *Aust. Met. Mag.*, 56, 241-266, 2007.

668 Osinski, R., Lorenz, P., Kruschke, T., Voigt, M., Ulbrich, U., Leckebusch, G. C., Faust, E., Hofherr, T., and  
669 Majewski, D.: An approach to build an event set of European windstorms based on ECMWF EPS, *Nat.*  
670 *Hazards Earth Syst. Sci.*, 16, 255-268, 10.5194/nhess-16-255-2016, 2016.

671 Ritchie, E. A., and Holland, G. J.: Scale interactions during the formation of Typhoon Irving, *Mon Weather Rev*,  
672 125, 1377-1396, 1997.

673 Roberts, M. J., Camp, J., Seddon, J., Vidale, P. L., Hodges, K., Vanniere, B., Mecking, J., Haarsma, R., Bellucci,  
674 A., Scoccimarro, E., Caron, L.-P., Chauvin, F., Terray, L., Valcke, S., Moine, M.-P., Putrasahan, D.,  
675 Roberts, C., Senan, R., Zarzycki, C., and Ullrich, P.: Impact of Model Resolution on Tropical Cyclone  
676 Simulation Using the HighResMIP-PRIMAVERA Multimodel Ensemble, *J Climate*, 33, 2557-2583,  
677 10.1175/JCLI-D-19-0639.1, 2020.

678 Rumpf, J., Weindl, H., Höppe, P., Rauch, E., and Schmidt, V.: Stochastic modelling of tropical cyclone tracks,  
679 *Mathematical Methods of Operations Research*, 66, 475-490, 10.1007/s00186-007-0168-7, 2007.

680 Rumpf, J., Weindl, H., Höppe, P., Rauch, E., and Schmidt, V.: Tropical cyclone hazard assessment using model-  
681 based track simulation, *Nat Hazards*, 48, 383-398, 10.1007/s11069-008-9268-9, 2009.

682 Sajjad, M., and Chan, J. C. L.: Risk assessment for the sustainability of coastal communities: A preliminary study,  
683 *Science of The Total Environment*, 671, 339-350, <https://doi.org/10.1016/j.scitotenv.2019.03.326>, 2019.

684 Sajjad, M., Chan, J. C. L., and Kanwal, S.: Integrating spatial statistics tools for coastal risk management: A case-  
685 study of typhoon risk in mainland China, *Ocean & Coastal Management*, 184, 105018,  
686 <https://doi.org/10.1016/j.ocecoaman.2019.105018>, 2020.

687 Shi, P.: On the role of government in integrated disaster risk governance—Based on practices in China,  
688 *International Journal of Disaster Risk Science*, 3, 139-146, 10.1007/s13753-012-0014-2, 2012.

689 Smith, A., Lott, N., and Vose, R.: The Integrated Surface Database: Recent Developments and Partnerships, *B*  
690 *Am Meteorol Soc*, 92, 704-708, 10.1175/2011BAMS3015.1, 2011.

691 Smith, A. B., and Katz, R. W.: US billion-dollar weather and climate disasters: data sources, trends, accuracy and  
692 biases, *Nat Hazards*, 67, 387-410, 10.1007/s11069-013-0566-5, 2013.

693 Smith, A. B., and Matthews, J. L.: Quantifying uncertainty and variable sensitivity within the US billion-dollar  
694 weather and climate disaster cost estimates, *Nat Hazards*, 77, 1829-1851, 10.1007/s11069-015-1678-x,  
695 2015.

696 Strachan, J., Vidale, P. L., Hodges, K., Roberts, M., and Demory, M.-E.: Investigating Global Tropical Cyclone  
697 Activity with a Hierarchy of AGCMs: The Role of Model Resolution, *J Climate*, 26, 133-152,  
698 10.1175/JCLI-D-12-00012.1, 2013.

699 Sun, B., Guo, C., and Cornelis van Kooten, G.: Hedging weather risk for corn production in Northeastern China:  
700 The efficiency of weather-indexed insurance, *Agricultural Finance Review*, 74, 555-572, 10.1108/AFR-  
701 01-2014-0001, 2014.

702 Swinbank, R., Kyouda, M., Buchanan, P., Froude, L., Hamill, T. M., Hewson, T. D., Keller, J. H., Matsueda, M.,  
703 Methven, J., Pappenberger, F., Scheuerer, M., Tittley, H. A., Wilson, L., and Yamaguchi, M.: The TIGGE  
704 Project and Its Achievements, *B Am Meteorol Soc*, 97, 49-67, 10.1175/BAMS-D-13-00191.1, 2015.

705 Swiss Re: Natural catastrophes and man-made disasters in 2015: Asia suffers substantial losses.  
706 [https://reliefweb.int/sites/reliefweb.int/files/resources/sigma1\\_2016\\_en.pdf](https://reliefweb.int/sites/reliefweb.int/files/resources/sigma1_2016_en.pdf), 2016.

707 Vickery, P. J., Skerlj, P. F., and Twisdale, L. A.: Simulation of Hurricane Risk in the U.S. Using Empirical Track  
708 Model, *Journal of Structural Engineering*, 126, 1222-1237, 10.1061/(ASCE)0733-  
709 9445(2000)126:10(1222), 2000.

710 Vitart, F., Prates, F., Bonet, A., and Sahin, C.: New tropical cyclone products on the web, *ECMWF Newsletter*,  
711 130, 2012.

712 Walz, M. A., and Leckebusch, G. C.: Loss potentials based on an ensemble forecast: How likely are winter  
713 windstorm losses similar to 1990?, *Atmos Sci Lett*, 20, e891, 10.1002/asl.891, 2019.

714 WMO: Typhoon Committee Operational Manual, World Meteorological Organization, World Meteorological  
715 Organization, 2019.

716 Wu, C.-C.: Typhoon Morakot: Key Findings from the Journal TAO for Improving Prediction of Extreme Rains  
717 at Landfall, *B Am Meteorol Soc*, 94, 155-160, 10.1175/BAMS-D-11-00155.1, 2012.

718 Xu, W., Qi, L., Du, Y., and Xia, L.: Analysis on Abnormal Tropical Cyclone Track Forecast Error of Ecmwf-Iifs  
719 in the Western North Pacific, *Tropical Cyclone Research and Review*, 5, 12-22,  
720 <https://doi.org/10.6057/2016TCRRh1.02>, 2016.

721 Yamaguchi, M., Vitart, F., Lang, S. T. K., Magnusson, L., Elsberry, R. L., Elliott, G., Kyouda, M., and Nakazawa,  
722 T.: Global Distribution of the Skill of Tropical Cyclone Activity Forecasts on Short- to Medium-Range  
723 Time Scales, *Weather and Forecasting*, 30, 1695-1709, 10.1175/WAF-D-14-00136.1, 2015.

724 Ye, T., Wang, Y., Wu, B., Shi, P., Wang, M., and Hu, X.: Government Investment in Disaster Risk Reduction  
725 Based on a Probabilistic Risk Model: A Case Study of Typhoon Disasters in Shenzhen, China,  
726 *International Journal of Disaster Risk Science*, 7, 123-137, 10.1007/s13753-016-0092-7, 2016.

727 Ye, T., Li, Y., Gao, Y., Wang, J., and Yi, M.: Designing index-based livestock insurance for managing snow  
728 disaster risk in Eastern Inner Mongolia, China, *International Journal of Disaster Risk Reduction*, 23, 160-  
729 168, 10.1016/j.ijdr.2017.04.013, 2017.

730 Zhang, X., Chen, G., Yu, H., and Zeng, Z.: Verification of Ensemble Track Forecasts of Tropical Cyclones During  
731 2014, *Tropical Cyclone Research and Review*, 4, 79-87, <https://doi.org/10.6057/2015TCRR02.04>, 2015.

732

733

734 **Tables**

Centre	Number of members	Runs per day	Resolution	Implementation date	Forecast lead time (hr)
CMA	14	2 (00, 12 UTC)	0.5625°×0.5625°	20070515	240
		2 (00, 12 UTC)		20140805	360
ECMWF	50	2 (00, 12 UTC)	0.5625°×0.5625°	20061001	360
JMA	50	1 (12 UTC)	1.25° × 1.25°	20060301	216
	50	1 (12 UTC)		20130328	264
	26	2 (0, 12 UTC)		20140226	264
NCEP	20	4 (0, 6, 12, 18 UTC)	1.0° × 1.0°	20070327	384

735

736 **Table 1.** Information of selected data sources from TIGGE archive.

737

Variables
Time average of area of cluster
Time average of longitude of cluster centre
Time average of latitude of cluster centre
Time average of maximum extent of cluster
Time average of mean wind speed
Time average of standard deviation of wind speed
Time average of minimum wind speed
Time average of maximum wind speed
Time average of longitude of location of maximum wind
Time average of latitude of location of maximum wind
Time average of storm severity index (SSI)
Standard deviation of time series of area of cluster
Standard deviation of time series of longitude of cluster centre
Standard deviation of time series of latitude of cluster centre
Standard deviation of time series of maximum extent of cluster
Standard deviation of time series of mean wind speed
Standard deviation of time series of standard deviation of wind speed
Standard deviation of time series of minimum wind speed
Standard deviation of time series of maximum wind speed
Standard deviation of time series of longitude of location of maximum wind
Standard deviation of time series of latitude of location of maximum wind
Standard deviation of time series of storm severity index
Number of 6-hourly time steps
Area of windstorm event footprint
Event SSI
Difference of latitude between the initial and final locations
Difference of longitude between the initial and final locations
Total distance travelled

738

739

740

741

**Table 2.** List of explanatory variables which are initially considered in the LRC model. can be obtained from the WiTRACK output.

Variable	t-value
Difference of latitude between the initial and final locations	12.5707
Difference of longitude between the initial and final locations	9.9983
Time average of standard deviation of wind speed	9.3709
Time average of minimum wind speed	8.5015
Time average of maximum extent of cluster	5.1416
Number of 6-hourly time steps	4.8719
Standard deviation of times series of latitude of location of maximum wind	3.4302
Standard deviation of times series of mean wind speed	2.3640
Standard deviation of times series of area of cluster	2.2447
Event SSI	1.9621
Standard deviation of times series of maximum extent of cluster	1.7922
Time average of latitude of cluster centre	1.4493
Standard deviation of time series of SSI	0.9980
Standard deviation of times series of longitude of location of maximum wind	0.9237
Standard deviation of times series of standard deviation of wind speed	0.7268
Time average of longitude of location of maximum wind	0.4204
Standard deviation of time series of minimum wind speed	0.2613

742

743 **Table 3.** List of explanatory variables and their associated t-value which are used in the construction of LRC.

744



Year	IBTrACS	CMA	ECMWF	JMA	NCEP	JRA-55
2008	21	19	19	19	17	10
2009	22	20	20	20	14	10
2010	13	13	13	13	13	6
2011	21	19	20	17	19	14
2012	24	23	23	23	23	16
2013	29	28	28	27	28	15
2014	19	12	17	17	17	13
2015	22	20	21	20	21	17
2016	26	25	25	24	25	13
2017	30	28	29	23	29	9
Total	227	207	215	203	206	123
Detection Rate		91.2%	94.7%	89.4%	90.7%	54.2%

745

746

747

748

749

**Table 4.** (From the left) Annual nNumber of historical TCs in IBTrACS (second column); Annual number of historical TCs detected in the respective forecast models with at least one MEPS counterpart identified (third to sixth columns); Annual number of historical TCs detected in JRA-55 (seventh column).

Centres	Number of TC windstorms	Number of Pure EPS TCs	% of TC windstorms as pure EPS TCs
CMA	39535	13322	33.7
ECMWF	215737	74091	34.3
JMA	56537	14964	26.5
NCEP	203903	96052	47.1

750

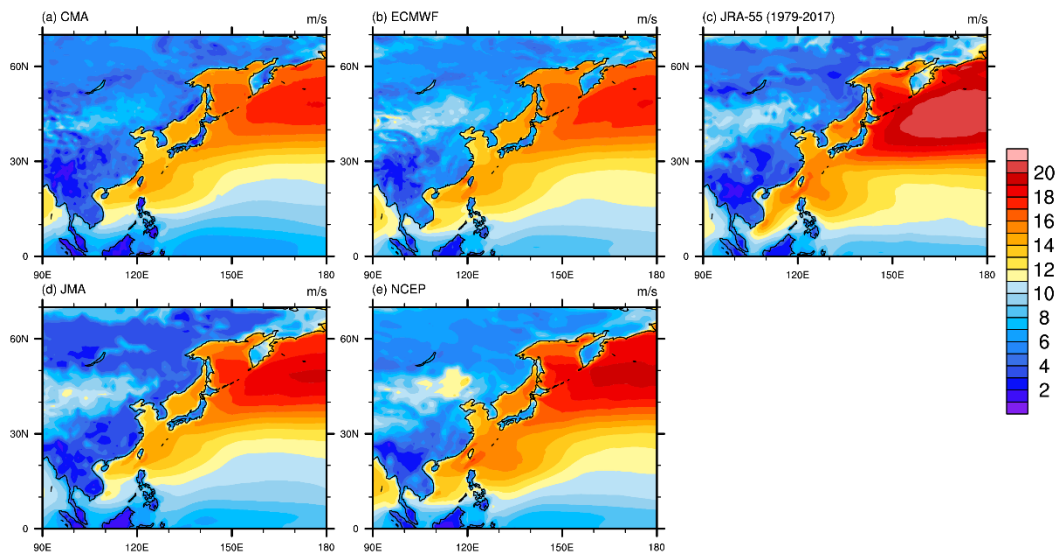
751 **Table 5.** Statistics of TCs in the selected TIGGE data.

752

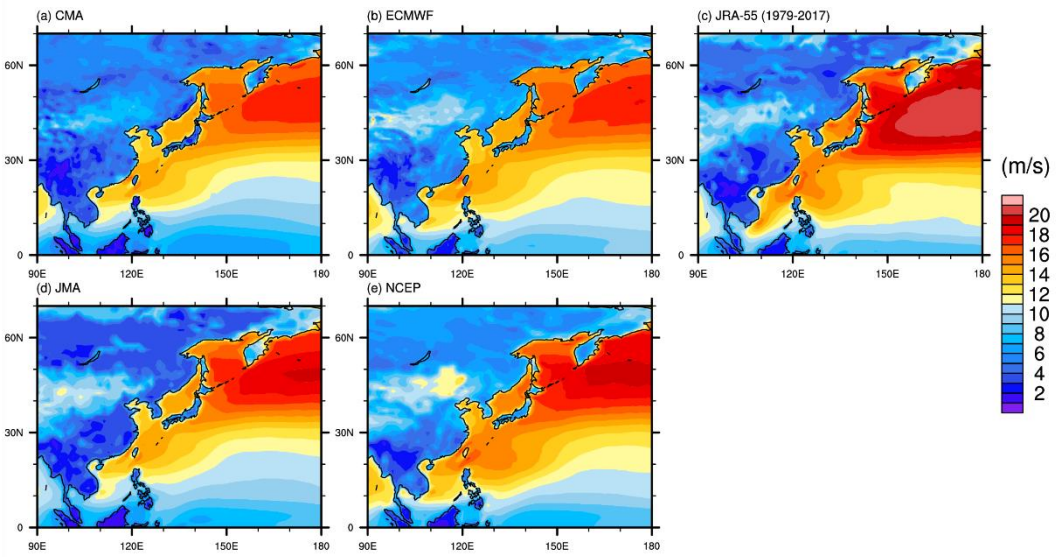
Intensity Class	IBTrACS	JRA-55	TPEPS
TD&TS	252	32	27643
STS	208	126	70759
TY	231	254	69794
VSTY	231	193	23686
VTY	85	63	6547
Total	1007	668	198429

753

754 **Table 6.** Number of TC records in IBTrACS, JRA-55 TC event set, and TPEPS TC event set, for different  
755 intensity classes. The classes are Tropical Depression (TD) and Tropical Storm (TS), Severe Tropical Storm  
756 (STS), Typhoon (TY), Very Strong Typhoon (VST), and Violent Typhoon (VTY). The intensity classes for  
757 IBTrACS are defined according to WMO (2019). The intensity classes for JRA-55 TC and TPEPS TC are derived  
758 from the WMO (2019) intensity classes by using quantile mapping of intensity records of JRA-55 TC and  
759 IBTrACS records.



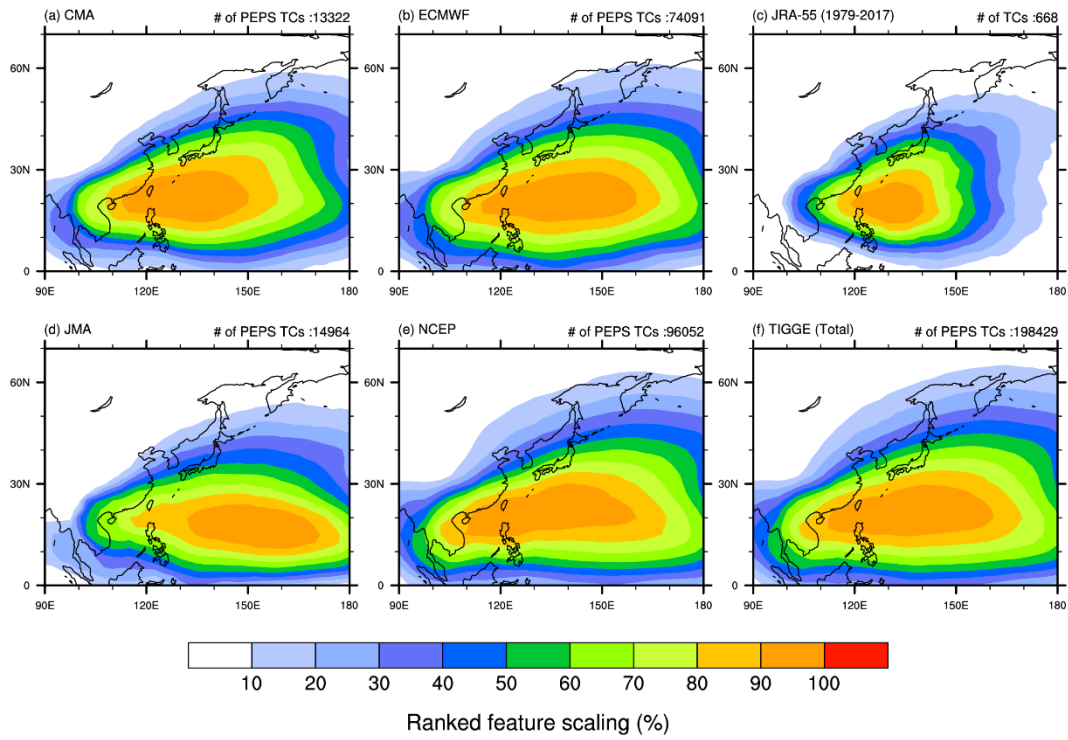
761



762

763 **Figure 1. Local 98<sup>th</sup> percentile wind speed for each grid box in the region for TIGGE: (a) CMA, (b) ECMWF, (d)**  
764 **JMA, (e) NCEP, and (c) JRA-55.**

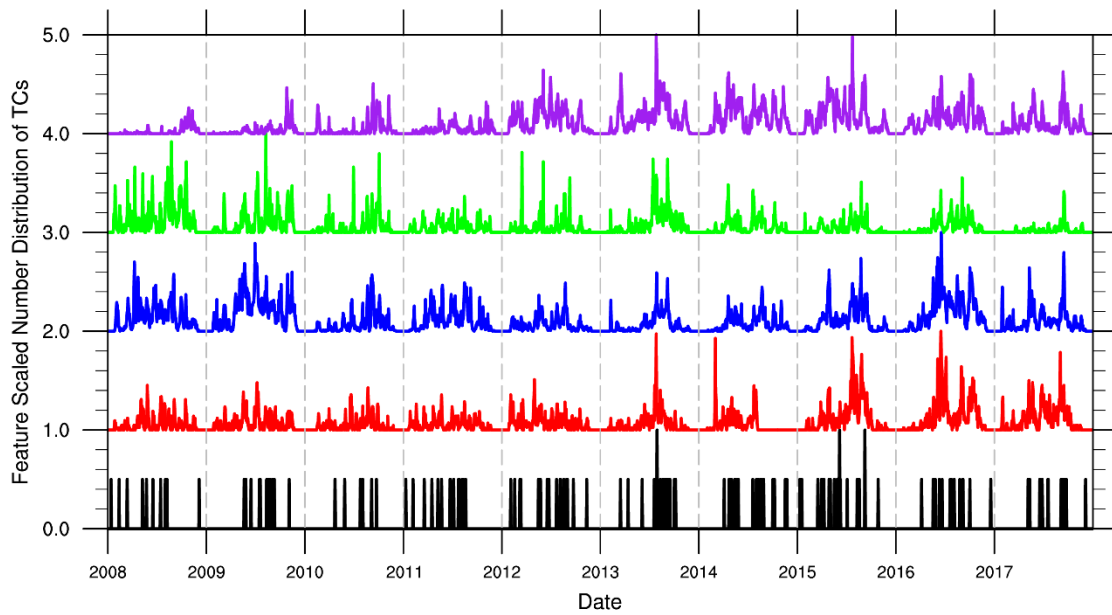
765



766

767 **Figure 2.** Ranked feature scaled track density (%) of different data sets: (a) CMA, (b) ECMWF, (c) JRA-55, (d)  
 768 JMA, (e) NCEP, and (f) TIGGE total. Number of TCs in the corresponding event set is stated on the top right of  
 769 each panel.

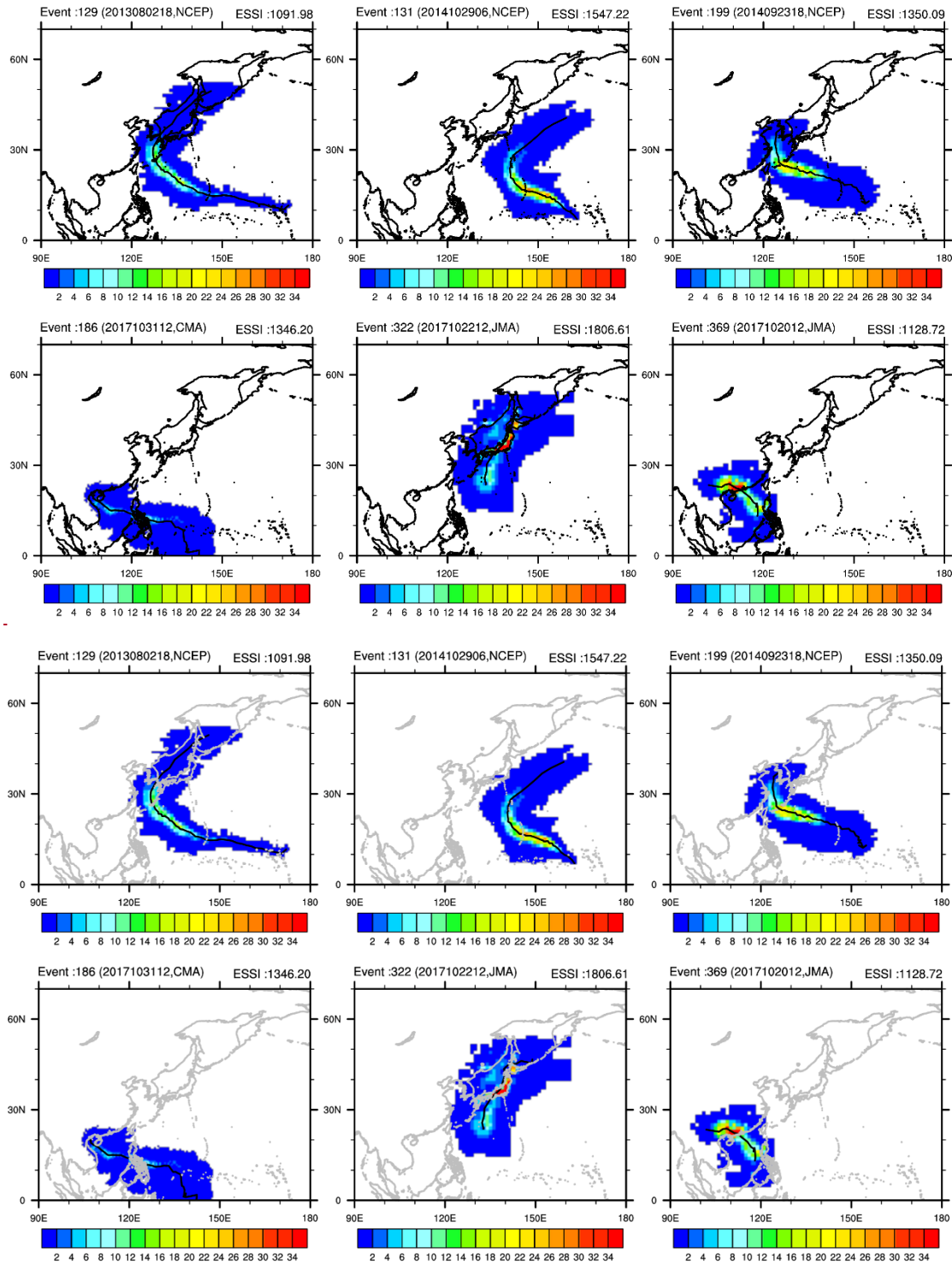
770



771

772 **Figure 3.** Feature scaled time series of number of TCs, which are first identified in each day formation in the of  
 773 TPEPS TC event set (CMA: red, ECMWF: blue, JMA: green, NCEP: purple) and JRA-55 event set (black). For  
 774 visual convenience, the time series of CMA, ECMWF, JMA, and NCEP are shifted by 1, 2, 3, 4, respectively.

775

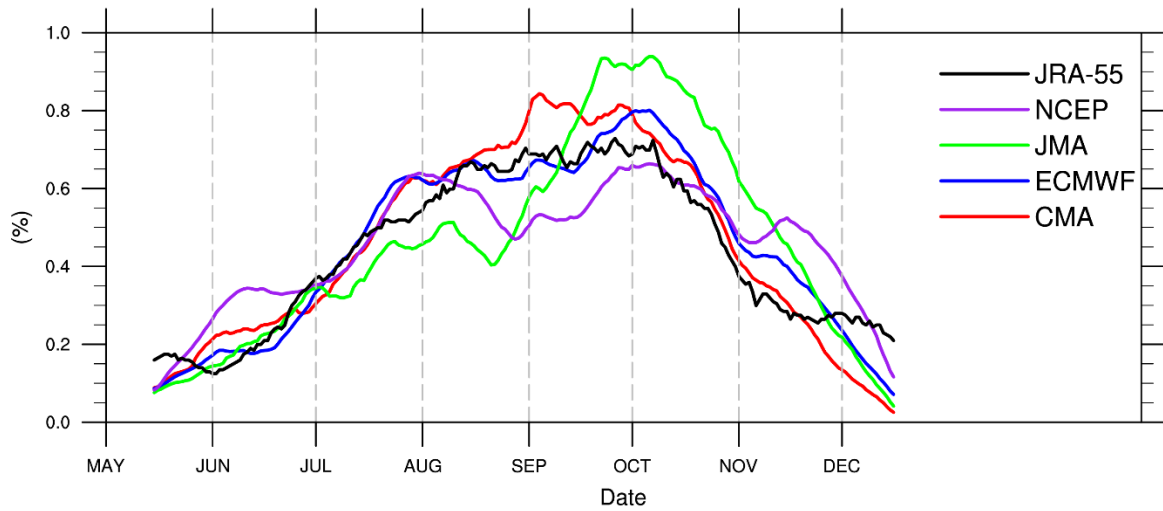


776

777

778 **Figure 4.** Some of the PEPS TC impact footprint (colour contours) and tracks (black line within the colour  
 779 contours) of the TPEPS TC event sets. The colour contours show the cumulative SSI of the PEPS TCs over their  
 780 respective lifetime at individual grid box. ESSI of each PEPS TC is shown on the top right of each panel.

781

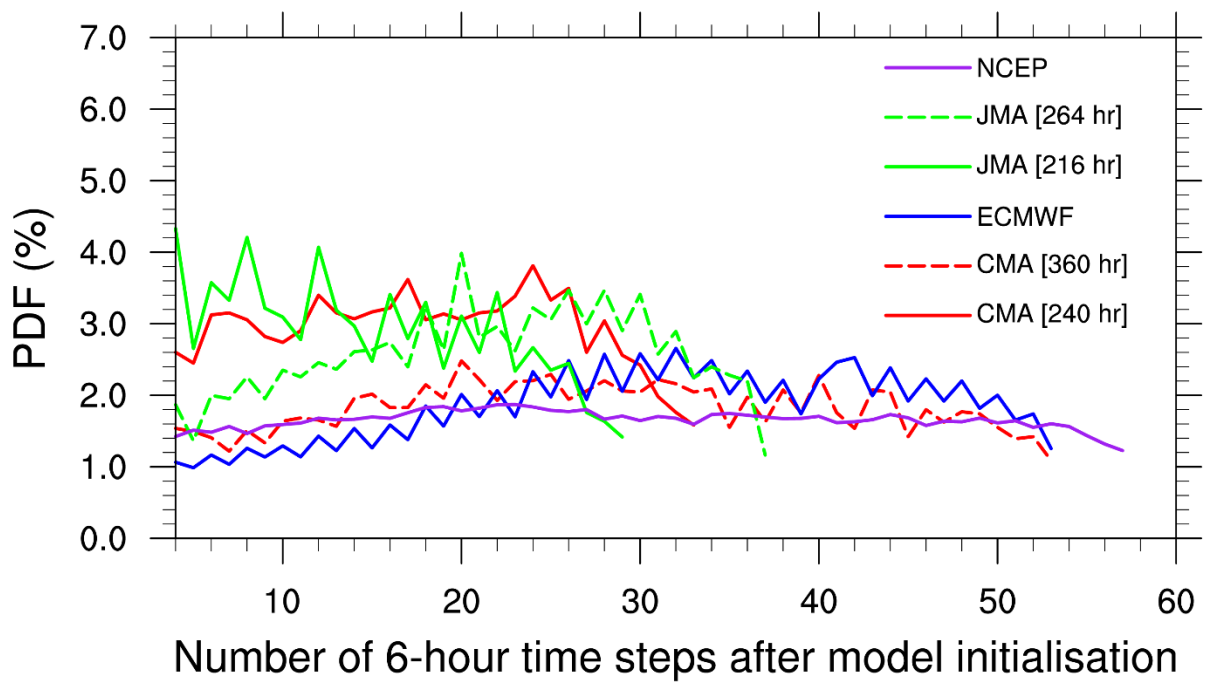


782

783 **Figure 5.** Climatological daily number distribution of TC first detection for TPEPS TC event set (CMA: red,  
 784 ECMWF: blue, JMA: green, NCEP: purple) and JRA-55 event set (black), i.e. the probability of TC being first  
 785 detected at a given day in the model. 30-day moving average is used in order to remove high frequency signal.

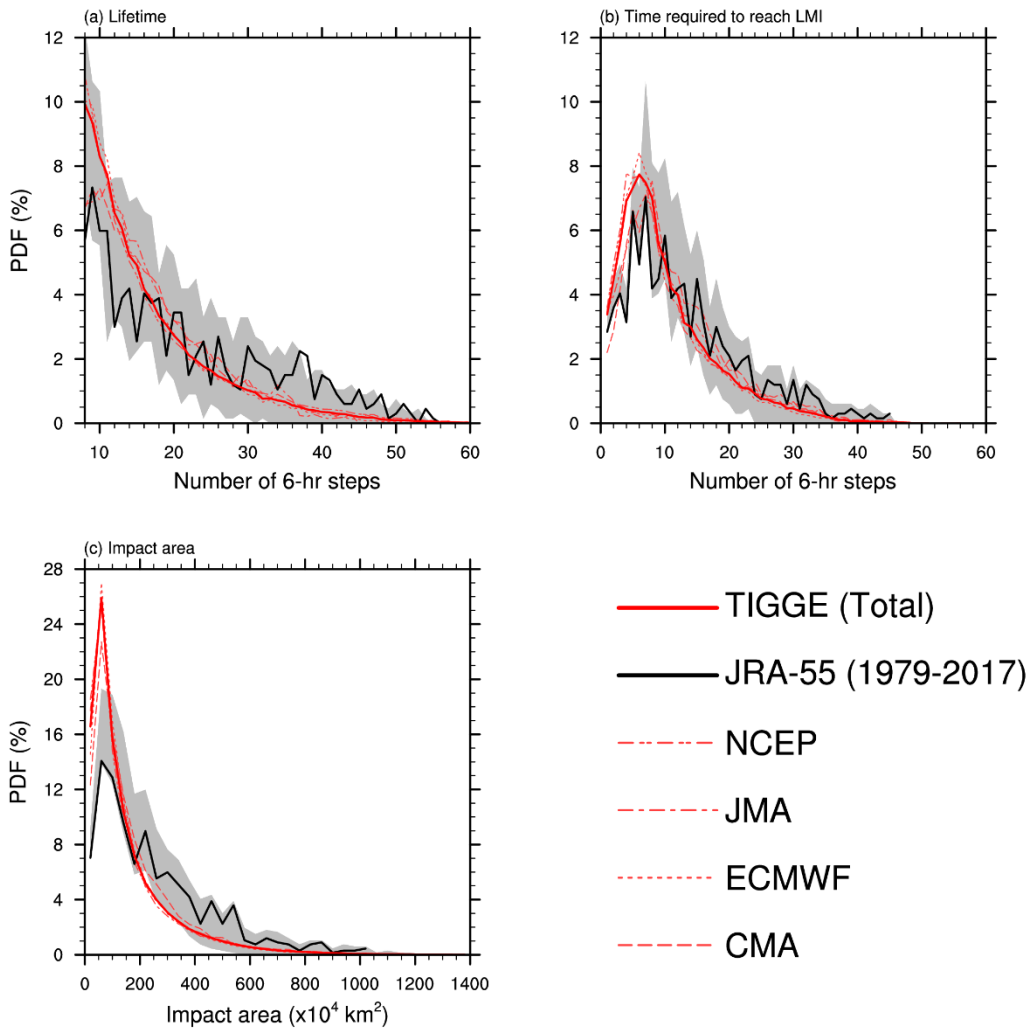
786





787

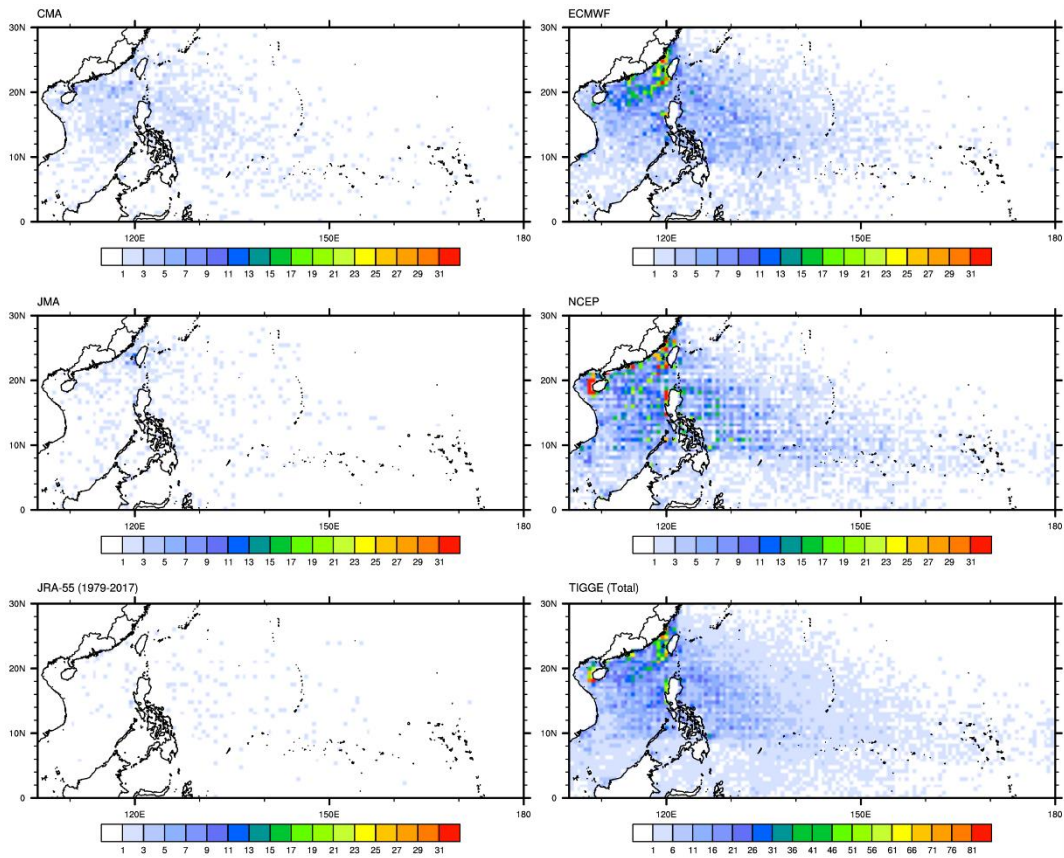
788 **Figure 6.** Temporal evolution of frequency of first storm detections of TPEPS event set (CMA: red, ECMWF:  
 789 blue, JMA: green, NCEP: purple).



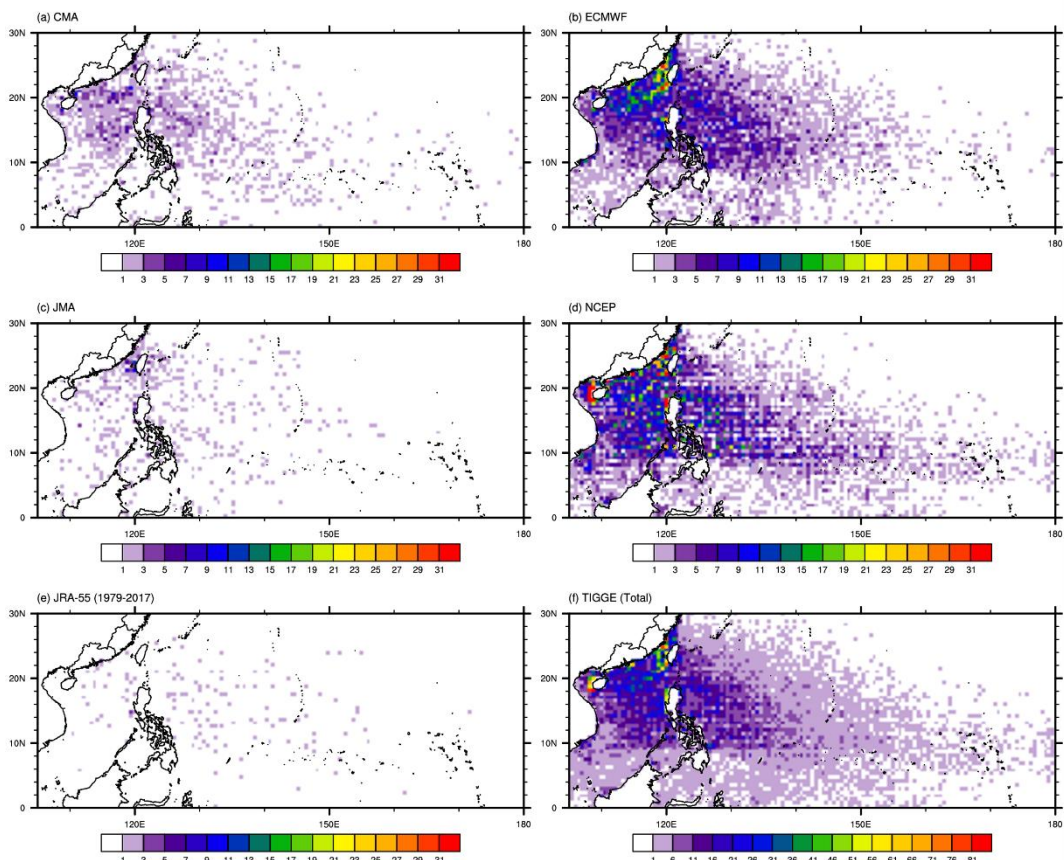
790

791 **Figure 7.** The distribution of (a) lifetime, (b) time required to reach LMI, and (c) impact area of TCs in TPEPS  
 792 TC event set (red lines) and JRA-55 event set (black line). The grey area indicates the spread of the lifetime  
 793 distribution of JRA-55 if finite simulation windows are applied to the JRA-55 event set.

794

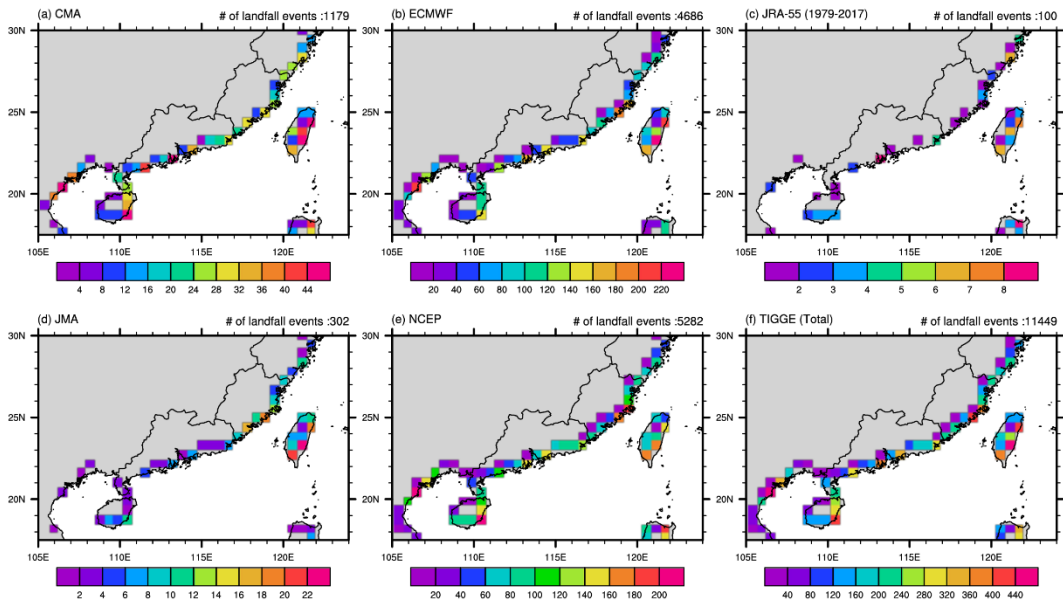


795



796

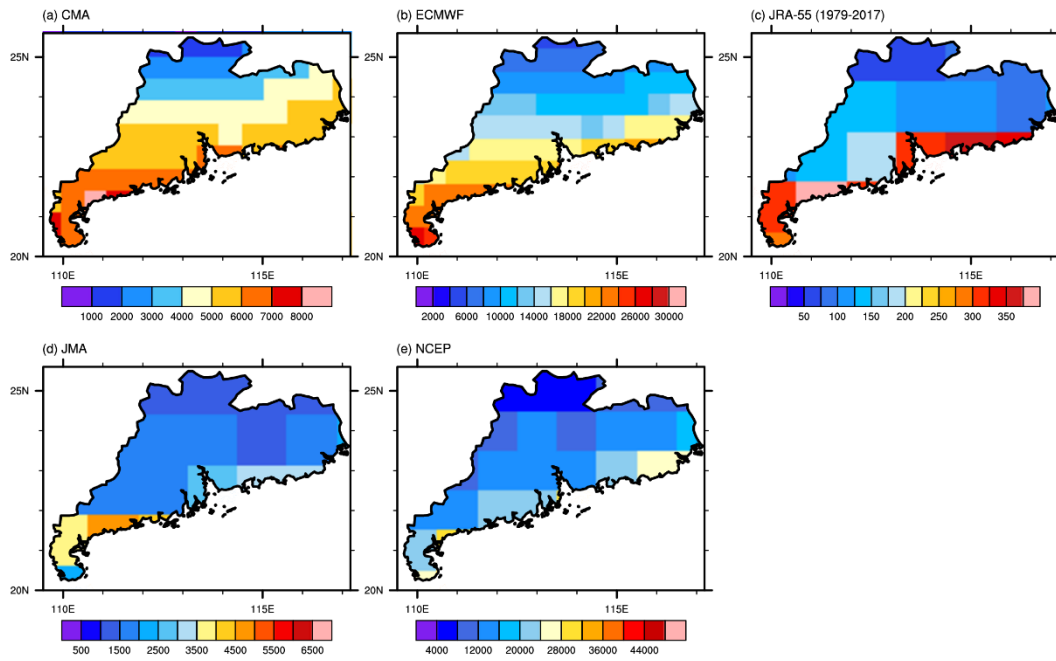
797 **Figure 8.** The spatial distribution of location of first detection of TCs (with LMI at least typhoon strength) which  
798 made landfall within the domain 105-180 °E, 0-30 °N for TPEPS TC event set and JRA-55 event set.  
799



800

801 **Figure 9.** Spatial distribution of number of landfall events (landfall with at least typhoon strength) for TPEPS TC  
 802 event sets and JRA-55 event set (colours). The total number of landfall events in each panel is shown on the top  
 803 right of each panel.

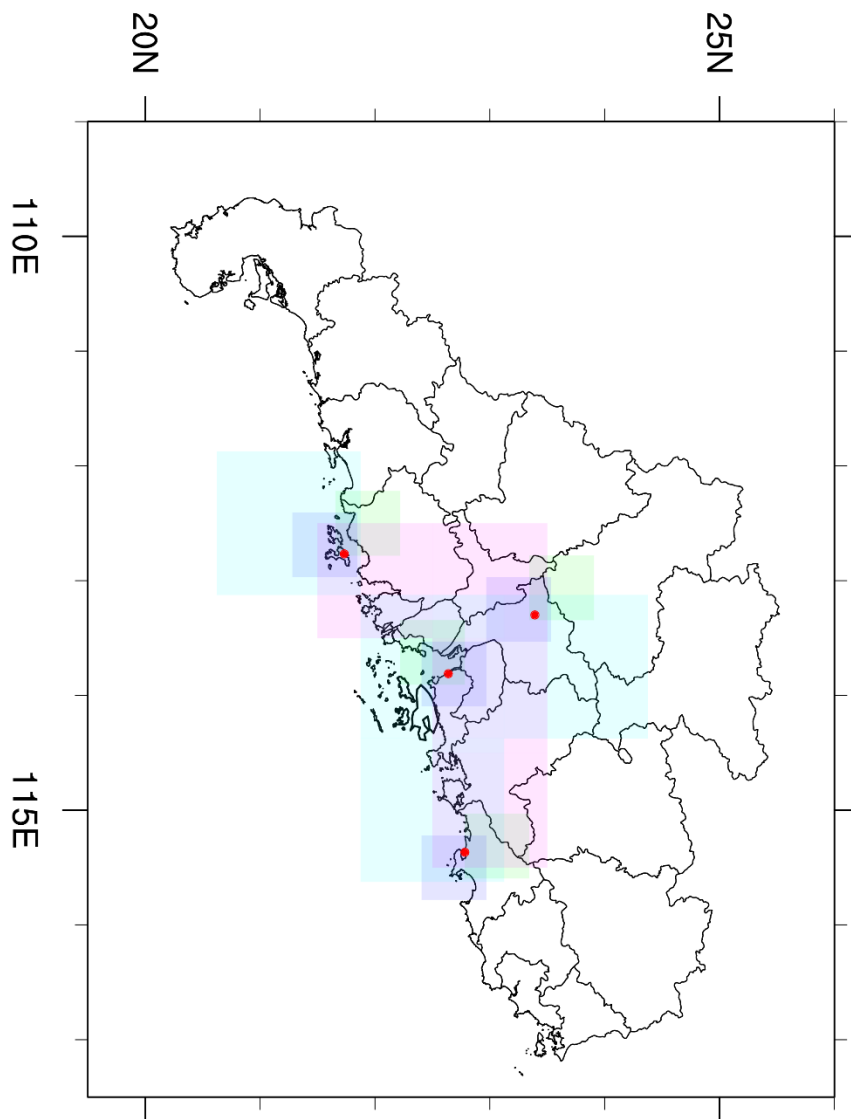
804



805

806 **Figure 10.** Number of TC-related 6-hourly data entries in each of the grid box in Guangdong Province, China,  
 807 for TPEPS TC event sets and JRA-55 event set.

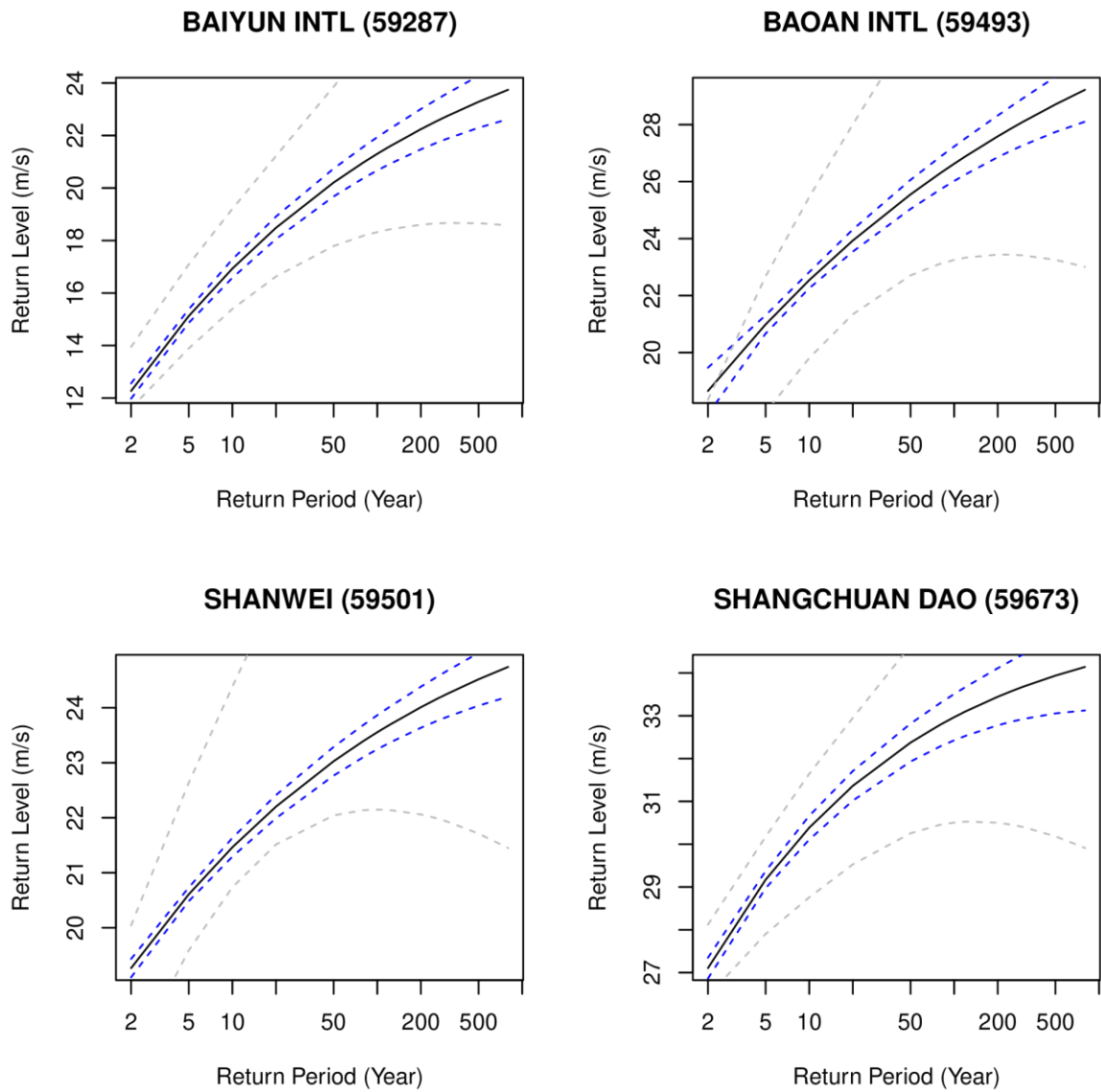
808



809

810 **Figure 11.** Locations of the selected surface observation stations (red dots) in Guangdong, China with  
 811 corresponding grid boxes from 4 EPS outputs: CMA (green), ECMWF (blue), JMA (cyan), and NCEP (magenta).  
 812 Information of prefectural boundaries is obtained from GADM version 3.6 Level 2 (available at  
 813 <https://gadm.org/data.html>)

814



815

816 **Figure 12.** Return period-return level plot for 4 selected surface observation stations: Baiyun International Airport,  
 817 Baoan International Airport, Shanwei, and Shangchuan Dao. Black lines indicate the best estimate of return  
 818 period-return level. Blue lines indicate the 95% confidence interval calculated using TIGGE PEPS event set.  
 819 Grey lines indicate the 95% confidence interval calculated using in situ observations.